

1 This paper is a non-peer reviewed preprint submitted to *EarthArXiv*. The manuscript was  
2 submitted to *Geophysical Research Letters* for peer review. Future updates on this manuscript  
3 will be provided once it's peer-reviewed or accepted. Please feel free to contact me at:  
4 [shiche@oregonstate.edu](mailto:shiche@oregonstate.edu) if you have any questions or feedbacks.

5

6

7    **Scaling High-resolution Soil Organic Matter Composition to Improve Predictions**  
8    **of Potential Soil Respiration Across the Continental United States**

9  
10   Cheng Shi<sup>a</sup>, Maruti Mudunuru<sup>b</sup>, Maggie Bowman<sup>c</sup>, Qian Zhao<sup>c</sup>, Jason Toyoda<sup>c</sup>, Will Kew<sup>c</sup>, Yuri Corilo<sup>c</sup>, Odeta  
11   Qafoku<sup>c</sup>, John R. Bargar<sup>c</sup>, Satish Karra<sup>c</sup>, & Emily B. Graham<sup>d,e\*</sup>

12  
13   <sup>a</sup>Oregon State University, Department of Biological & Ecological Engineering, Corvallis, OR, United States.

14   <sup>b</sup>Energy and Environment Directorate, Pacific Northwest National Laboratory, Richland, WA, United States.

15   <sup>c</sup>Environmental Molecular Science Laboratory, Pacific Northwest National Laboratory, Richland, WA, United  
16   States.

17   <sup>d</sup>Earth and Biological Sciences Directorate, Pacific Northwest National Laboratory, Richland, WA, United States.

18   <sup>e</sup>School of Biological Sciences, Washington State University, Pullman, WA, United States.

19  
20   \*Corresponding author: [emily.graham@pnnl.gov](mailto:emily.graham@pnnl.gov)

21  
22   Key points:

- 23        • Dissolved SOM composition improves predictions of potential soil respiration  
24        • Machine learning extracts key molecules from complex high-resolution SOM profiles  
25        • Surface soil respiration was better predicted by dissolved SOM than subsoil respiration

26

## 27 **Abstract**

28  
29 Despite the importance of microbial respiration of soil organic matter (SOM) in regulating carbon  
30 flux between soils and atmosphere, soil carbon cycling models remain primarily based on climate  
31 and soil properties, leading to large uncertainty in predictions. With data from the 1000 Soils Pilot  
32 of the Molecular Observation Network (MONet), we analyzed high resolution water-extractable  
33 SOM profiles from standardized soil cores across the United States to address this knowledge gap.  
34 Our innovation lies in using machine learning to distill the thousands of SOM formula into  
35 tractable units; and it enables integrating data from molecular measurements into soil respiration  
36 models. In surface soils, SOM chemistry provided better estimates of potential soil respiration than  
37 soil physicochemistry, and using them combined yielded the best prediction. Overall, we identify  
38 specific subsets of organic molecules that may improve predictions of global soil respiration and  
39 create a strong basis for developing new representations in process-based models.

40

## 41 **Plain Language Summary**

42 Soil organic carbon (C) is one of the largest and most active pools in the global carbon cycle.  
43 Microbial decomposition of soil organic matter (SOM) – the primary constituent of soil C –  
44 releases a tremendous amount of carbon dioxide (CO<sub>2</sub>) to the atmosphere. This process is soil  
45 microbial respiration. To evaluate if SOM composition can improve predictions of soil respiration,  
46 we collected soil cores from across the continental US, and analyzed both standardized soil  
47 biogeochemistry and molecular composition of water-extractable SOM, as part of the Molecular  
48 Observation Network (MONet). We developed machine learning (ML) based workflow to extract  
49 key SOM signatures and used the SOM signatures to assess the added value of molecular  
50 information to predict soil respiration, compared to standard soil physicochemistry data. The  
51 results suggested that SOM molecular composition improved the prediction accuracy of soil  
52 respiration in surface soils, where most soil carbon is stored. In deeper soils, the model  
53 performance was not improved, possibly due to the greater importance of mineral-associated SOM  
54 below the surface layer. Our results identified key SOM molecules in predicting soil respiration  
55 and supported the significance of SOM dynamics in future development of soil carbon cycling  
56 models.

## 57 **Introduction**

58 Soil respiration is estimated to release 60-100 Gt of carbon (C) to the atmosphere per year  
59 (Giardina et al., 2014; Jian et al., 2021), six to ten times as much C as released by fossil fuel  
60 combustion (~10 Gt C (Friedlingstein et al., 2022)). Microbial respiration of soil organic matter  
61 (SOM) is one of the most important contributors to soil carbon dioxide (CO<sub>2</sub>) emissions and a  
62 critical link in the global C cycle (Graham & Hofmockel, 2022). With increasing temperatures  
63 under climate change, soil C repositories are vulnerable to increased rates of microbial  
64 respiration (Lei et al., 2021; Melillo et al., 2017; Nissan et al., 2023), which can lead to positive  
65 feedbacks in global CO<sub>2</sub> emissions and temperature rises (Bond-Lamberty & Thomson, 2010).  
66 Despite decades of research, soil C fluxes remain one of the largest uncertainties in global  
67 climate predictions (Mark A Bradford et al., 2016; Crowther et al., 2016; Davidson & Janssens,  
68 2006; Todd-Brown et al., 2014; Warner et al., 2019). Novel molecular measurements have  
69 recently been applied to identify SOM composition in an effort to understand molecular-scale  
70 processes that could improve model predictions of CO<sub>2</sub> fluxes (Bahureksa et al., 2021; Billings et  
71 al., 2021; Liang et al., 2019; Sanderman et al., 2021). Despite these efforts, our attempts to  
72 improve soil C model predictions by refining chemical pools have yielded mixed results (Cotrufo  
73 et al., 2013; Robertson et al., 2019; Sulman et al., 2014).

74  
75 The interplay of factors such as soil moisture, pH, nutrients, mineralogy, and SOM concentration  
76 and chemistry governs microbially-derived transformations of SOM (Amador & Jones, 1993;  
77 Ciais et al., 2014; Curiel Yuste et al., 2007; Falloon et al., 2011); but these relationships are  
78 difficult to constrain (Billings & Ballantyne IV, 2013; Graham & Hofmockel, 2022). The most  
79 commonly used modeling approaches are based on Raich's model, which estimates respiration  
80 primarily as a function of temperature and water availability (Raich & Potter, 1995; Raich et al.,  
81 2002). Newer process-based model formulations use an additional suite of physical and  
82 biogeochemical measurements to represent microbial and mineral processes. They incorporate  
83 SOM chemistry either through several discrete pools or through their thermodynamic properties  
84 (Kyker-Snowman et al., 2020; Waring et al., 2020; Wieder et al., 2018). With large  
85 spatiotemporal heterogeneity and limited availability of comprehensive and standardized  
86 measurements at regional-to-continental scales, accurate predictions of microbial SOM  
87 decomposition across different ecosystems remain challenging (Mark A. Bradford et al., 2021).

88

89 A better understanding of SOM concentration, composition, and bioavailability may enhance our  
90 ability to predict soil C cycling processes through their controls on soil respiration and related  
91 enzymatic activities (Kyker-Snowman et al., 2020; Robertson et al., 2019; Song et al., 2020;  
92 Waring et al., 2020; Wieder et al., 2018). Yet, we have little ability to extract meaningful  
93 information from the thousands of molecules detected by state-of-science measurements.  
94 Variations in the bioavailability of chemical classes of SOM are mediated by geochemical  
95 conditions and biophysical constraints, such as microbial biomass and necromass, reactive  
96 metals and minerals, organic and mineral horizon thickness, and other climate-related variables  
97 (Hall et al., 2020). For example, coarse-textured soil is more conducive to decomposition of  
98 chemically labile litter-derived C potentially due to higher fungal activity in organic-rich  
99 horizons (Huys et al., 2022; Scott et al., 1996). In addition, the interface between fresh litter  
100 inputs and soil minerals can serve as a hotspot for microbial breakdown of C found in the litter,  
101 resulting in the formation of soil aggregates and organo-mineral associations (Witzgall et al.,  
102 2021). This variability underlines the essential need to identify unique subsets of SOM formula  
103 that contribute more to soil respiration among different ecosystems and soil depths.

104

105 Although high mass resolution measurements can provide unprecedented characterization of the  
106 thousands of individual formulae that comprise SOM, the interpretation of these data types  
107 largely remains guided by coarse chemical and ecological groupings. Unsupervised machine  
108 learning models that summarize large data into a small number of significant features have been  
109 widely used to study microbial ecology, SOM composition, and other environmental problems  
110 with multidimensional data (Sonnewald et al., 2020). Here, we develop models using semi-  
111 supervised machine learning (non-negative matrix factorization with custom  $k$ -means clustering,  
112 NMF $k$ ) to reduce the complexity of molecular information into  $k$  distinct signatures of water-  
113 extractable SOM chemistry at two depths in cores collected across the continental United States.  
114 We then explore the extent to which these signatures and NMF $k$ -enabled feature set can provide  
115 additional insight into rates of soil respiration beyond variables that are more routinely collected.  
116 Our novel workflow results in a 1,000-fold decrease in SOM pool complexity, and the extracted  
117 SOM signatures can improve predictions of soil potential respiration across soils from vastly  
118 different ecosystems. This enables data from state-of-science measurement techniques to be

119 filtered into the molecules that most directly explain soil respiration. Our workflow is applicable  
120 to multiple types of mass spectrometry data and to studies ranging from localized experiments to  
121 global surveys.

## 122 **Methods**

123

### 124 *Soil sampling and characterization.*

125

126 As part of the 1000 Soils Pilot study for the Molecular Observation Network (MONet) program,  
127 we collected 66 soils from across the continental US using standardized sampling procedures  
128 described by Bowman et al. (2023) (Figure S1). Two long cores (30 cm) and three short cores  
129 (10 cm) were collected at each site. We also conducted field measurements, including soil  
130 temperature, volumetric water content, vegetation type, and weather conditions. Cores were  
131 shipped on ice overnight to the Pacific Northwest Laboratory for further analysis. A full  
132 description of sampling and analytical methodologies is available in Supporting Information and  
133 Bowman et al. (2023).

134

### 135 *Water extractable SOM characterization.*

136

137 We extracted water-soluble SOM from soils using solid phase extraction and analyzed using a  
138 Bruker 7-T Fourier transform ion cyclotron resonance mass spectrometry (FTICR MS) at the  
139 Environmental Molecular Sciences Laboratory (EMSL) in Richland, WA. More details on SOM  
140 extraction methods and FTICR MS analysis are in Supporting Information and Bowman et al.  
141 (2023). Raw FTICR MS data was processed with CoreMS (Python package, installed on  
142 2022/11/22) (Corilo et al., 2021), including signal processing, peak detection, and molecular  
143 formula assignment (Supporting Information). We predicted compound classes of the filtered  
144 formulae based on O/C and H/C ratios of van Krevelen classes (Kim et al., 2003; Tfaily et al.,  
145 2015). The suffix “-like” in chemical classes indicates the uncertainty of the van Krevelen  
146 classification method (Tfaily et al., 2015). We converted the peak intensity values to  
147 present/absent (1/0) and separated the final dataset by soil depth (surface vs. subsoil) for  
148 statistical analysis. Alpha diversity was calculated as the total number of SOM formulae  
149 identified in each sample.

150

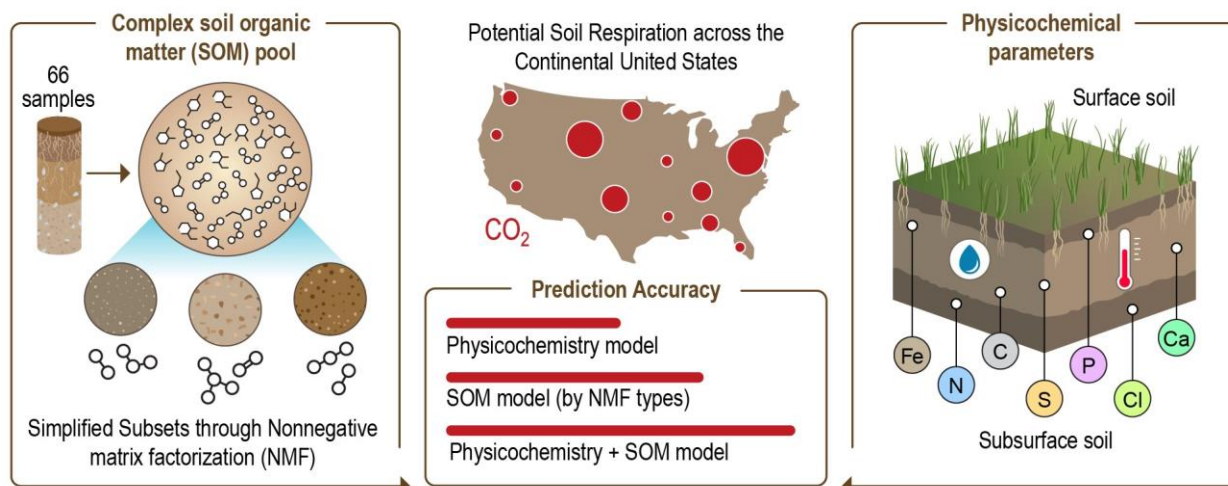
151 *Data analysis and machine learning methods.*

152

153 We used linear regression models to evaluate the relationship between soil potential respiration  
154 and soil physicochemical variables (Supporting Information). To avoid the impacts of different  
155 magnitudes of the data that might lead to biased relationships, we performed  $\log_{10}$  transformation  
156 on potential respiration rates, total C, total N, total sulfur, and Mn concentration.

157

158 We used non-negative matrix factorization with custom k-means clustering (NMF $k$ ) (Bhattarai et  
159 al., 2020) to identify signature components from the 7312 and 5515 SOM molecular formula (for  
160 surface and subsoil, respectively) we detected (i.e.,  $N$  formulae in  $m$  soils) with *pyNMF $k$*  package  
161 (Python, <https://github.com/lanl/pyDNMFk>, Figure 1). More details on NMF $k$  assumptions,  
162 model settings, and model robustness are in the Supporting Information. Briefly, NMF $k$  tends to  
163 be more successful at extracting explainable basis or signatures from large multivariate datasets,  
164 compared to other dimensionality reduction tools such as principal component analysis  
165 (Devarajan, 2008; D. Lee & Seung, 2000). As applied here, NMF $k$  summarizes data into discrete  
166 signatures that contain weights for each SOM formulae detected by FTICR MS for each soil  
167 layer independently (i.e., a separate set of signatures was generated to summarize surface versus  
168 subsoils, allowing us to explore depth-specific relationships with potential soil respiration). The  
169 optimal number of signatures was determined from silhouette coefficients of different NMF $k$   
170 models. A  $W$ -matrix with the weights of each SOM formulae ( $N$ ) to each extracted signature ( $k$ ),  
171 and an  $H$ -matrix with the contribution of each signature ( $k$ ) to each soil sample ( $m$ ) were  
172 generated from NMF $k$ .



173

174 *Figure 1. Workflow: Machine learning models summarize molecular data to predict soil respiration.*  
 175 *Non-negative matrix factorization (NMFk) extracts key SOM signatures from high resolution mass*  
 176 *spectrometry measurements of SOM. Gradient boosting regression predicts soil respiration with*  
 177 *physicochemistry, SOM signatures, and physicochemistry combined with SOM signatures.*

178

179 To define groups of soils with high, medium, or low rates of potential respiration, we used *k*-  
 180 means clustering on potential soil respiration (Figure S2) with the elbow method to select the  
 181 number of groups (*KMeans* from *scikit-learn* package) (Bholowalia & Kumar, 2014). Then, we  
 182 mapped the extracted *k* signatures to soil respiration using supervised machine learning. To  
 183 evaluate the potential value of NMFk-extracted SOM signatures for explaining soil respiration,  
 184 we conducted three sets of machine learning models: (1) selected environmental parameters  
 185 alone (i.e., variables with  $R^2 > 0.2$  in individual regression, Table S1), (2) SOM composition  
 186 alone (NMFk weights from H-matrix), and (3) environmental and SOM composition in  
 187 combination. All machine learning models were built using gradient boosting regression (GBR)  
 188 from *scikit-learn* package (v 0.24, Python). More details in model training, testing and validation  
 189 are in Supporting Information.

190

## 191 **Results**

### 192 *Soil physicochemistry and potential respiration*

193

194 Overall, many soil parameters, including potential soil respiration, tended to be higher in surface  
 195 soils than in subsoils. Significant differences ( $p < 0.05$ ) between surface soils and subsoils in total



196 C, total N, total sulfur, C/N ratio, and other factors are shown Figures S3 and S4. In particular,  
197 surface soils had higher potential respiration rates (median: 72.6 ug CO<sub>2</sub>/g soil/day) than subsoils  
198 (median: 21.9 ug CO<sub>2</sub>/g soil/day) (Mann–Whitney U = 3022.5, N<sub>surface</sub> = 63, N<sub>subsoil</sub> = 61, p <  
199 0.05).

200

201 For both surface and subsoils, soil with high potential respiration tended to be sourced from the  
202 Midwestern and Northeastern United States. (Figure S5). In surface soil, high potential  
203 respiration was associated with five soils collected in Utah, Wyoming, and Virginia (within  
204 temperate conifer forest and temperate broadleaf & mixed forest biomes, Figure S1, Figure S5).  
205 In subsoils, high respiration was associated with three soils from Utah and Maryland (temperate  
206 conifer forests and broadleaf & mixed forests biomes). Desert soils had the lowest respiration in  
207 both layers (Figure S1).

208

209 We found relationships between soil respiration and many variables that supported prevailing  
210 paradigms (Figure S4). A full correlation table of associations between different soil properties is  
211 available in the SI (Table S1). Briefly, potential respiration rates in both surface and subsoils  
212 were positively correlated with gravimetric water content (GWC) ( $r^2$ : 0.246 and 0.225) and  
213 cation exchange capacity (CEC,  $r^2$ : 0.405 and 0.354). They were also positively correlated with  
214 total C and total N content, with stronger relationships in surface soils ( $r^2$ : 0.487 vs. 0.268 for  
215 total C,  $r^2$ : 0.439 v.s. 0.248 for total N). Total bases and magnesium (Mg) concentrations had a  
216 higher correlation to respiration in subsoils than surface soils ( $r^2$ : 0.227 v.s. 0.146 and 0.287 vs.  
217 0.160), while manganese (Mn) concentrations were correlated to respiration in surface soils ( $r^2$ :  
218 0.324).

219

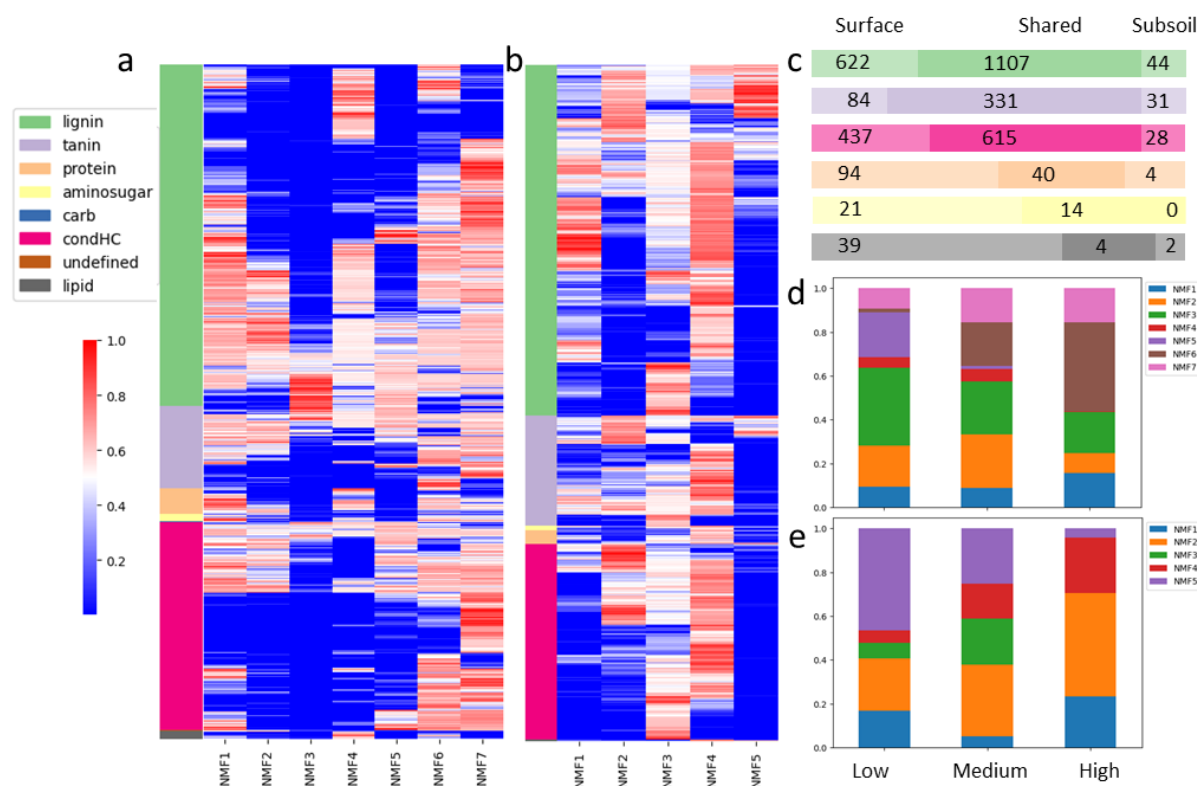
220 *SOM composition and NMFk partitioning of SOM.*

221

222 Across all soils, the most common chemical classes of SOM were lignin-, condensed  
223 hydrocarbon-, and tannin-like formula. Most formula in these classes were present in both  
224 surface and subsoils (i.e., ‘shared’ formula). However, surface soils contained more unique  
225 formula than subsoils for all compound classes (Figure S5c). In particular, many protein-, amino  
226 sugar-, and lipid-like compounds were identified in surface soils only, with very few compounds

227 in these classes being unique to subsoils. Soils from the Midwestern U.S. and the West Coast had  
 228 relatively higher alpha diversity than soils from other regions (Figure S5a).

229  
 230 Then, we used NMF $k$  to summarize SOM composition into 7 and 5 NMF $k$  signatures,  
 231 respectively, for surface and subsoils (Figure 2). Geographic patterns in SOM signatures are  
 232 displayed in Figure S6-7, with more geographic clustering of NMFs in surface soils than in  
 233 subsoils. The most important formula contributing to the composition of each NMF (i.e., formula  
 234 with normalized weights >0.5 in W-matrix) are shown in Figure 2a-b. NMF-selected formula  
 235 (weights >0.5 in W-matrix) generally followed the same general patterns as the overall SOM  
 236 pool but showed amplified relationships (Figure 2c).



237  
 238  
 239 *Figure 2. NMF $k$  partitioning of SOM composition. (a-b) Relative contribution of organic formula to each*  
 240 *SOM signature identified by NMF $k$  in a) surface and b) subsoils. The color in each cell represents the*  
 241 *normalized (0 to 1) relative contribution for each SOM formula (row) to each NMF $k$  signature (column).*  
 242 *Red indicates the most important contributor, and blue indicates the least. The side bar indicates the*  
 243 *compound class of each SOM formula. (c) The number of shared and unique formula identified as*  
 244 *important (normalized weights >0.5) by NMF $k$  in surface and subsoils. (d-e) The relative contribution of*  
 245 *NMF $k$  signatures to each level of potential respiration in both d) surface and e) subsoils. Surface soils:*

246 *low respiration (N = 44), medium respiration (N = 14), high respiration (N = 5). Subsoils: low*  
247 *respiration (N = 48), medium respiration (N = 10), high respiration (N = 3).*

248

249 For surface soils, NMF1, 4, 6, and 7 had a relatively high number of important compounds  
250 identified as lignin-like. NMF6 and 7 had large contributions of condensed hydrocarbon-like  
251 formula. NMF1 had high contribution from protein-like and amino sugar-like compounds, while  
252 NMF3 and 5 had the lowest contribution from protein-like, amino sugar-like, and lipid-like  
253 compounds of any NMF. NMF4 had the largest number of lipid-like compounds as important  
254 features relative to any other surface soil NMF.

255

256 In subsoil samples, important formula for all NMFs tended to be classified as lignin-, tannin-,  
257 and/or condensed hydrocarbon-like. NMF1 and NMF5 had a larger fraction of features identified  
258 as lignin-like compounds than other NMFs in subsoils. NMF2 and NMF3 had a larger fraction of  
259 condensed hydrocarbon-like compounds than other NMFs, while NMF4 had large contributions  
260 of protein-like and amino sugar-like formula (Figure S8).

261

262 We also observed differences in the dominant NMF signatures across high-, medium-, and low-  
263 respiration soils, particularly in surface soils (Figure 2d-e). High respiration surface soils were  
264 characterized by five NMF signatures (1, 2, 3, 6, and 7), with the largest contribution from  
265 NMF6. Low respiration surface soils, in contrast, uniquely contained NMF5, and they did not  
266 have any contribution from NMF6. In subsoils, high respiration soils had high contribution of  
267 NMF3 and 4, while low respiration soils were disproportionately associated with NMF5.

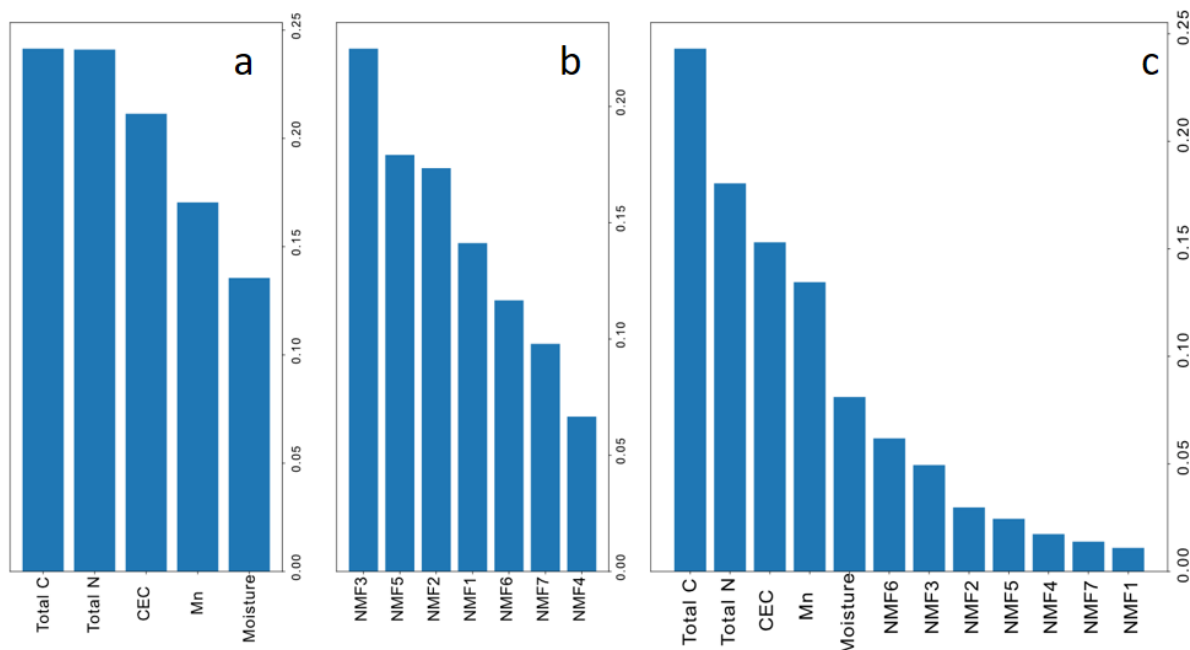
268

269 *Relative importance of physicochemistry and SOM composition in potential soil respiration*  
270 *models*

271

272 We developed gradient-boosting regression models to predict potential soil respiration with (1)  
273 physicochemical variables, (2) SOM composition represented by NMF $k$  signatures, and (3) both  
274 of them combined. Model performances are summarized in Table S2 and Figure 3.

275



276  
 277 *Figure 3. Relative importance of each predictor in surface soil potential respiration models. a) Model*  
 278 *with physicochemical variables only. b) Model with SOM signatures represented by NMFs only. c) Model*  
 279 *with both physicochemical variables and SOM signatures.*

280  
 281 Selected physicochemical variables (consisting of total C, total N, CEC, moisture, Mn (surface),  
 282 total base (subsoil), and Mg (subsoil) concentration) had significant independent Pearson's  
 283 correlation to respiration w/  $p < 0.05$  and  $r^2 > 0.2$  (Table S1). Physicochemical variables  
 284 predicted potential respiration rates in surface and subsoils equally well ( $R^2 = 0.44$  and  $0.43$   
 285 respectively for testing data). In surface soils, total C, total N, and cation exchange capacity  
 286 (CEC) were identified as the top 3 most important predictors, followed by Mn concentration and  
 287 soil moisture (Figure 3). In subsoils, CEC, total N, and soil moisture were the most important  
 288 predictor, and total C was the least important predictor (Figure S9).

289  
 290 Using SOM composition (NMF signatures) as predictors, we had better model performance in  
 291 surface soils than in subsoils (testing  $R^2 = 0.54$  vs.  $0.08$ ), and SOM composition alone predicted  
 292 more slightly variation in potential respiration rates than physicochemical variables alone in  
 293 surface soils (testing  $R^2 = 0.54$  vs.  $0.44$ ), even when controlling for an equal number of  
 294 predictors (testing  $R^2 = 0.48$  vs.  $0.44$ ). NMF3, NMF5, and NMF2 were the most important SOM  
 295 composition variables for explaining soil respiration in surface soils (Figure 3).

296  
297 When we combined both physicochemical variables and SOM composition into a single  
298 predictor set, we obtained better respiration model performance ( $R^2 = 0.62$ ) compared to models  
299 with environmental variables or SOM composition in surface soils only. However, the model  
300 describing potential respiration rates in subsoil was worse ( $R^2 = 0.36$ ) when compared to models  
301 based on physicochemical variables only. In surface soils, the 3 most important variables were  
302 the same as the physicochemical model. NMF6 was identified as the most important SOM  
303 variable, followed by NMF3, NMF2, and NMF5 (Figure 3).

304

## 305 **Discussion**

### 306 *Depth partitioning in relationships between SOM composition and potential soil respiration*

307 Given that not all chemical constituents of SOM contribute to soil respiration and that surface  
308 and subsoils differ substantially in mineralogy and structure, we hypothesized that distinct  
309 subsets of SOM would contribute to respiration in surface vs. subsoils. More details on SOM  
310 chemistry and potential soil respiration are available in the Supplemental Information.

311  
312 There was no single NMF that dominated low- vs. high-potential respiration soils in either layer,  
313 however, NMF weightings varied substantially across soils with different rates of potential  
314 respiration in both layers (Figure 2d-e). This suggests that different subsets of SOM were  
315 disproportionately associated with soils exhibiting high vs. low potential respiration rates. While  
316 patterns in SOM chemical across geographic regions were difficult to disentangle, the spatial  
317 distribution of NMF types suggested local similarity in SOM composition in both layers (Figure  
318 S6-7), likely reflecting similar underlying chemistry, mineralogy, and/or biogeochemical  
319 processes (Brye et al., 2016).

320

321 The distillation of multidimensional SOM composition profiles into a tractable set of formula  
322 that influence soil respiration is a key challenge in soil ecology (Billings et al., 2021; Garayburu-  
323 Caruso et al., 2020; Graham et al., 2018; Turețcaia et al., 2023). The SOM formula within NMFs  
324 that correspond to changes in soil respiration may represent a key step forward in understanding  
325 the chemical bioavailability of water-extractable organic matter in soils; and our approach can be

326 used with multiple different extraction types and/or high-resolution mass spectrometry  
327 measurements. Our results are particularly promising for surface soils, where the dissolved SOM  
328 pool (e.g., water-extractable SOM) is thought to fuel microbial respiration. The comparatively  
329 weak relationship between subsoil water-extractable SOM and potential soil respiration as  
330 compared to surface soils highlights recent work emphasizing the importance of mineral-  
331 associated organic matter in soil C storage (Benbi et al., 2014; Cotrufo et al., 2019; Lugato et al.,  
332 2021). We therefore suggest that combining our analytical workflow with measurements on  
333 mineral-associated organic matter specifically would increase our understanding of SOM cycling  
334 in deeper soil layers.

335  
336 In surface soils, NMF6 displayed a dramatic increase in weighting from low-to-high respiration  
337 soils. It contained a diverse suite of compounds including protein-, (soluble) lipid-, and amino  
338 sugar-like formula that can be rapidly used as microbial substrate. Proteins and amino sugars in  
339 particular can bolster microbial metabolism of SOM (Campbell et al., 2022; Hernández &  
340 Hobbie, 2010), thus the prevalence of these compounds within NMF6 may support high potential  
341 rates of soil respiration. NMF1 and NMF7 in surface soils contained a diverse mixture of  
342 compounds and also increased from low-to-high respiration soils, supporting a possible  
343 relationship between SOM pool diversity and microbial respiration (see previous section). In  
344 contrast, surface NMF2, NMF3 and NMF5 decreased in importance from low-to-high respiration  
345 soils and primarily consisted of a small but unique subset of lignin- and tannin-like compounds  
346 (Figure 2a). This is consistent with low bioavailability of its chemical constituents suppressing  
347 microbial respiration (Kögel-Knabner, 2002; Marschner & Kalbitz, 2003). It suggests that  
348 despite the often-inferred high bioavailability of water-extractable SOM (Garayburu-Caruso et  
349 al., 2020), there may be a significant fraction of water-extractable SOM that is chemically  
350 protected from microbial decomposition (Garayburu-Caruso et al., 2020; Hernández & Hobbie,  
351 2010; Tureçcaia et al., 2023). Interestingly, NMF4 in surface soils — which contained the  
352 greatest number of lipid-like formula (Figure 2a) and had a comparatively large fraction of  
353 protein-like formula — was not present in any high-respiration soils. We therefore suggest that  
354 NMF4 may be an indicator of non-living microbial biomass (i.e., necromass) which is  
355 disproportionately comprised of lipids (microbial cell wall remnants) and amino sugars and  
356 proteins (the basis of intracellular materials) (Angst et al., 2021; Camenzind et al., 2023).

357  
358 While these results are broadly consistent with contemporary understanding of the behavior of  
359 coarse groups of SOM chemistries, there is substantial variation in SOM bioavailability within  
360 most chemical classes of SOM. NMF<sub>k</sub> provides specific subsets of molecules that correspond to  
361 soil respiration of at the continental scale. It allows us to downscale from the thousands of  
362 molecules detectable by state-of-science methods into more tractable units for further  
363 investigation. This is a significant advance, as it allows for more detailed experimentation into  
364 and model representation of the precise chemical reactions that leading to the destabilization of  
365 SOM. Because the identified molecules are robust across a plethora of different ecosystems, we  
366 are hopeful that this workflow can advance generalizable knowledge on soil carbon cycling.

367  
368 *Relative importance of physicochemistry and SOM composition in predicting potential soil*  
369 *respiration*

370  
371 By developing machine learning models to predict respiration with soil physicochemistry and  
372 SOM composition (NMFs) separately and in combination, we were able to distinguish the  
373 contributions of each set of factors for predicting soil potential respiration. The models based on  
374 physicochemistry alone explained a modest amount of variation in soil respiration (44% and  
375 43% in surface and subsoils, respectively), in line with the range of explanatory power observed  
376 in other works (Allison, 2012; Graham et al., 2014).

377  
378 For surface soils, models based on SOM composition alone (54% variation explained) and both  
379 physicochemical factors and SOM composition combined (62% variation explained) suggest  
380 that SOM composition (1) can predict soil respiration at least as well as commonly measured  
381 physicochemical variables and (2) explains some portion of soil respiration that is not captured  
382 by physicochemistry. While physicochemical predictors were stronger predictors of soil  
383 respiration than SOM composition in the combined surface soil models, the inclusion of SOM  
384 composition improved physicochemistry-only models by 18%, indicating that it may  
385 significantly impact our ability to predict the rate of soil C cycling processes. NMF3 (which was  
386 mainly in low-respiration soil and was comprised of lignin- and tannin-like formula, see previous  
387 sections) in particular was the strongest predictor of soil respiration in models based on SOM

388 composition alone followed by NMF2 and NMF5. The relative chemical recalcitrance of the  
389 most important predictors of respiration may suggest that the proportion of thermodynamically  
390 unfavorable formula in water-extractable SOM has a direct inhibitory effect on soil metabolism.  
391 Indeed, thermodynamic regulation of organic C composition can be a key control for the rate of  
392 respiration in ecosystems (Garayburu-Caruso et al., 2020; Turețcaia et al., 2023). Therefore, the  
393 inclusion of SOM composition in more mechanistic modeling approaches may be able to  
394 improve predictions of soil respiration rates.

395  
396 However, models for subsoils displayed different dynamics. In the subsoil model based on  
397 physicochemical variables alone, total C was the least important predictor (vs. the most  
398 important predictor for surface soils), and the model containing SOM composition did not yield  
399 high predictive power. The partial dependence of soil respiration to total C was stronger in  
400 surface soil than in subsoil (Figure S10), which could explain why SOM composition did not add  
401 predictive power to potential respiration in subsoils. Since more total and organic C is stored in  
402 surface soils, resolution into the water-extractable SOM pool (reflected here by NMFs) might be  
403 a more significant factor for predicting surface soil respiration than in subsoils that are  
404 characterized by lower total C and more mineral-associated SOM (Rumpel & Kögel-Knabner,  
405 2011).

406  
407 Our results suggest that NMF-extracted signatures of SOM composition are able to improve  
408 surface soil model performance by integrating fundamental molecular information into soil  
409 respiration models across very different soil ecosystems at the continental scale. NMF6, which  
410 was the most important NMF signature in combined models of surface respiration, consisted of  
411 diverse chemically-bioavailable compounds, and it mainly existed in high-respiration soils (see  
412 previous sections) (Marschner & Kalbitz, 2003). We therefore suggest that chemically-  
413 bioavailable compounds in water-extractable SOM pools may provide the greatest  
414 complementary explanatory power to physicochemical factors in respiration predictions. Because  
415 SOM pools vary tremendously at the continental-scale, refined regional or local studies that  
416 encompass lower-variability parameter spaces may yield even more value of SOM molecular  
417 data to soil C modeling.

418



**419 Conclusion**

420 Leveraging molecular information of SOM chemistry to improve conceptualizations and models  
421 of soil C cycling is a pressing challenge for global biogeochemical and climate predictions. In  
422 this study, we use machine learning (NMF $k$ ) to distill the thousands of SOM molecules detected  
423 by ultrahigh resolution mass spectrometry into tractable units that are associated with microbial  
424 respiration. By evaluating soil cores collected across the continental United States, we show that  
425 these signatures of SOM composition represent subsets of SOM formula which differentially  
426 contribute to soils exhibiting low versus high rates of potential respiration. We then disentangle  
427 the SOM formula from each NMF $k$ -extracted signature and validate their chemical properties in  
428 the context of contemporary understandings of SOM bioavailability. Further, subsets of SOM  
429 chemistry identified by NMF $k$  explained a greater proportion of potential soil respiration than  
430 commonly measured physicochemical factors, and they provided additional explanatory power  
431 beyond these factors in combined models. Our results provide a basis for molecular information  
432 to spur the development of new process-based representations of soil C cycles and underscore  
433 the role of specific chemical constituents within the water-extractable SOM as determinants of  
434 soil respiration.

## 435 Acknowledgement

436 Soil data were provided by the Molecular Observation Network (MONet) at the Environmental  
 437 Molecular Sciences Laboratory (<https://ror.org/04rc0xn13>), a DOE Office of Science user  
 438 facility sponsored by the Biological and Environmental Research program under Contract No.  
 439 DE-AC05-76RL01830. The work (proposal: 10.46936/10.25585/60008970) conducted by the  
 440 U.S. Department of Energy, Joint Genome Institute (<https://ror.org/04xm1d337>), a DOE Office  
 441 of Science user facility, is supported by the Office of Science of the U.S. Department of Energy  
 442 operated under Contract No. DE-AC02-05CH11231.

443 The Molecular Observation Network (MONet) database is an open, FAIR, and publicly available  
 444 compilation of the molecular and microstructural properties of soil. Data in the MONet open  
 445 science database can be found at <https://sc-data.emsl.pnnl.gov/>.

446

## 447 References

- 448 Allison, S. (2012). A trait-based approach for modelling microbial litter decomposition. *Ecology letters*, *15*(9),  
 449 1058-1070.
- 450 Amador, J., & Jones, R. D. (1993). Nutrient limitations on microbial respiration in peat soils with different total  
 451 phosphorus content. *Soil Biology and Biochemistry*, *25*(6), 793-801.
- 452 Angst, G., Mueller, K. E., Nierop, K. G. J., & Simpson, M. J. (2021). Plant- or microbial-derived? A review on the  
 453 molecular composition of stabilized soil organic matter. *Soil Biology and Biochemistry*, *156*, 108189.  
 454 <https://www.sciencedirect.com/science/article/pii/S0038071721000614>
- 455 Bahureksa, W., Tfaily, M. M., Boiteau, R. M., Young, R. B., Logan, M. N., McKenna, A. M., & Borch, T. (2021).  
 456 Soil organic matter characterization by Fourier transform ion cyclotron resonance mass spectrometry  
 457 (FTICR MS): A critical review of sample preparation, analysis, and data interpretation. *Environmental*  
 458 *Science & Technology*, *55*(14), 9637-9656.
- 459 Benbi, D., Boparai, A., & Brar, K. (2014). Decomposition of particulate organic matter is more sensitive to  
 460 temperature than the mineral associated organic matter. *Soil Biology and Biochemistry*, *70*, 183-192.
- 461 Bhattarai, M., Chennupati, G., Skau, E., Vangara, R., Djidjev, H., & Alexandrov, B. S. (2020, 22-24 Sept. 2020).  
 462 *Distributed Non-Negative Tensor Train Decomposition*. Paper presented at the 2020 IEEE High  
 463 Performance Extreme Computing Conference (HPEC).
- 464 Bholowalia, P., & Kumar, A. (2014). EBK-means: A clustering technique based on elbow method and k-means in  
 465 WSN. *International Journal of Computer Applications*, *105*(9).
- 466 Billings, S. A., & Ballantyne IV, F. (2013). How interactions between microbial resource demands, soil organic  
 467 matter stoichiometry, and substrate reactivity determine the direction and magnitude of soil respiratory  
 468 responses to warming. *Global Change Biology*, *19*(1), 90-102.
- 469 Billings, S. A., Lajtha, K., Malhotra, A., Berhe, A. A., de Graaff, M. A., Earl, S., et al. (2021). Soil organic carbon is  
 470 not just for soil scientists: measurement recommendations for diverse practitioners. *Ecological*  
 471 *Applications*, *31*(3), e02290.
- 472 Bond-Lamberty, B., & Thomson, A. (2010). Temperature-associated increases in the global soil respiration record.  
 473 *Nature*, *464*(7288), 579-582.
- 474 Bowman, M. M., Heath, A. E., Varga, T., Battu, A. K., Chu, R. K., Toyoda, J., et al. (2023). One thousand soils for  
 475 molecular understanding of belowground carbon cycling. *Frontiers in Soil Science*, *3*. Perspective.  
 476 <https://www.frontiersin.org/articles/10.3389/fsoil.2023.1120425>

- 477 Bradford, M. A., Wieder, W. R., Bonan, G. B., Fierer, N., Raymond, P. A., & Crowther, T. W. (2016). Managing  
478 uncertainty in soil carbon feedbacks to climate change. *Nature Climate Change*, 6(8), 751-758.
- 479 Bradford, M. A., Wood, S. A., Addicott, E. T., Fenichel, E. P., Fields, N., González-Rivero, J., et al. (2021).  
480 Quantifying microbial control of soil organic matter dynamics at macrosystem scales. *Biogeochemistry*,  
481 156(1), 19-40. <https://doi.org/10.1007/s10533-021-00789-5>
- 482 Brye, K. R., McMullen, R. L., Silveira, M. L., Motschenbacher, J. M. D., Smith, S. F., Gbur, E. E., & Helton, M. L.  
483 (2016). Environmental controls on soil respiration across a southern US climate gradient: a meta-analysis.  
484 *Geoderma Regional*, 7(2), 110-119. <https://www.sciencedirect.com/science/article/pii/S2352009416300104>
- 485 Camenzind, T., Mason-Jones, K., Mansour, I., Rillig, M. C., & Lehmann, J. (2023). Formation of necromass-derived  
486 soil organic carbon determined by microbial death pathways. *Nature Geoscience*, 16(2), 115-122.  
487 <https://doi.org/10.1038/s41561-022-01100-3>
- 488 Campbell, T. P., Ulrich, D. E. M., Toyoda, J., Thompson, J., Munsky, B., Albright, M. B. N., et al. (2022).  
489 Microbial Communities Influence Soil Dissolved Organic Carbon Concentration by Altering Metabolite  
490 Composition. *Frontiers in microbiology*, 12. Original Research.  
491 <https://www.frontiersin.org/articles/10.3389/fmicb.2021.799014>
- 492 Ciais, P., Sabine, C., Bala, G., Bopp, L., Brovkin, V., Canadell, J., et al. (2014). Carbon and other biogeochemical  
493 cycles. In *Climate change 2013: the physical science basis. Contribution of Working Group I to the Fifth*  
494 *Assessment Report of the Intergovernmental Panel on Climate Change* (pp. 465-570): Cambridge  
495 University Press.
- 496 Corilo, Y., Kew, W., & McCue, L. (2021). EMSL-Computing/CoreMS: CoreMS 1.0.0 (v1.0.0). *Zenodo*10, 5281.
- 497 Cotrufo, M. F., Ranalli, M. G., Haddix, M. L., Six, J., & Lugato, E. (2019). Soil carbon storage informed by  
498 particulate and mineral-associated organic matter. *Nature Geoscience*, 12(12), 989-994.
- 499 Cotrufo, M. F., Wallenstein, M. D., Boot, C. M., Deneff, K., & Paul, E. (2013). The Microbial Efficiency-Matrix S  
500 tabilization (MEMS) framework integrates plant litter decomposition with soil organic matter stabilization:  
501 Do labile plant inputs form stable soil organic matter? *Global change biology*, 19(4), 988-995.
- 502 Crowther, T. W., Todd-Brown, K. E. O., Rowe, C. W., Wieder, W. R., Carey, J. C., Machmuller, M. B., et al.  
503 (2016). Quantifying global soil carbon losses in response to warming. *Nature*, 540(7631), 104-108.  
504 <https://doi.org/10.1038/nature20150>
- 505 Curiel Yuste, J., Baldocchi, D., Gershenson, A., Goldstein, A., Misson, L., & Wong, S. (2007). Microbial soil  
506 respiration and its dependency on carbon inputs, soil temperature and moisture. *Global Change Biology*,  
507 13(9), 2018-2035.
- 508 Davidson, E. A., & Janssens, I. A. (2006). Temperature sensitivity of soil carbon decomposition and feedbacks to  
509 climate change. *Nature*, 440(7081), 165-173.
- 510 Devarajan, K. (2008). Nonnegative Matrix Factorization: An Analytical and Interpretive Tool in Computational  
511 Biology. *PLOS Computational Biology*, 4(7), e1000029. <https://doi.org/10.1371/journal.pcbi.1000029>
- 512 Falloon, P., Jones, C. D., Ades, M., & Paul, K. (2011). Direct soil moisture controls of future global soil carbon  
513 changes: An important source of uncertainty. *Global Biogeochemical Cycles*, 25(3).
- 514 Friedlingstein, P., O'Sullivan, M., Jones, M. W., Andrew, R. M., Gregor, L., Hauck, J., et al. (2022). Global Carbon  
515 Budget 2022. *Earth Syst. Sci. Data*, 14(11), 4811-4900. <https://essd.copernicus.org/articles/14/4811/2022/>
- 516 Garayburu-Caruso, V. A., Stegen, J. C., Song, H.-S., Renteria, L., Wells, J., Garcia, W., et al. (2020). Carbon  
517 limitation leads to thermodynamic regulation of aerobic metabolism. *Environmental Science & Technology*  
518 *Letters*, 7(7), 517-524.
- 519 Giardina, C. P., Litton, C. M., Crow, S. E., & Asner, G. P. (2014). Warming-related increases in soil CO<sub>2</sub> efflux are  
520 explained by increased below-ground carbon flux. *Nature Climate Change*, 4(9), 822-827.  
521 <https://doi.org/10.1038/nclimate2322>
- 522 Graham, E. B., Crump, A. R., Kennedy, D. W., Arntzen, E., Fansler, S., Purvine, S. O., et al. (2018). Multi-omics  
523 comparison reveals metabolome biochemistry, not microbiome composition or gene expression,  
524 corresponds to elevated biogeochemical function in the hyporheic zone. *Science of the total environment*,  
525 642, 742-753.
- 526 Graham, E. B., & Hofmockel, K. S. (2022). Ecological stoichiometry as a foundation for omics-enabled  
527 biogeochemical models of soil organic matter decomposition. *Biogeochemistry*, 157(1), 31-50.
- 528 Graham, E. B., Wieder, W. R., Leff, J. W., Weintraub, S. R., Townsend, A. R., Cleveland, C. C., et al. (2014). Do  
529 we need to understand microbial communities to predict ecosystem function? A comparison of statistical  
530 models of nitrogen cycling processes. *Soil Biology and Biochemistry*, 68, 279-282.

- 531 Hall, S. J., Ye, C., Weintraub, S. R., & Hockaday, W. C. (2020). Molecular trade-offs in soil organic carbon  
532 composition at continental scale. *Nature Geoscience*, *13*(10), 687-692. [https://doi.org/10.1038/s41561-020-](https://doi.org/10.1038/s41561-020-0634-x)  
533 0634-x
- 534 Hernández, D. L., & Hobbie, S. E. (2010). The effects of substrate composition, quantity, and diversity on microbial  
535 activity. *Plant and Soil*, *335*(1), 397-411. <https://doi.org/10.1007/s11104-010-0428-9>
- 536 Huys, R., Poirier, V., Bourget, M. Y., Roumet, C., Hättenschwiler, S., Fromin, N., et al. (2022). Plant litter  
537 chemistry controls coarse-textured soil carbon dynamics. *Journal of Ecology*, *110*(12), 2911-2928.
- 538 Jian, J., Vargas, R., Anderson-Teixeira, K., Stell, E., Herrmann, V., Horn, M., et al. (2021). A restructured and  
539 updated global soil respiration database (SRDB-V5). *Earth Syst. Sci. Data*, *13*(2), 255-267.  
540 <https://essd.copernicus.org/articles/13/255/2021/>
- 541 Kim, S., Kramer, R. W., & Hatcher, P. G. (2003). Graphical method for analysis of ultrahigh-resolution broadband  
542 mass spectra of natural organic matter, the van Krevelen diagram. *Analytical chemistry*, *75*(20), 5336-5344.
- 543 Kögel-Knabner, I. (2002). The macromolecular organic composition of plant and microbial residues as inputs to soil  
544 organic matter. *Soil Biology and Biochemistry*, *34*(2), 139-162.  
545 <https://www.sciencedirect.com/science/article/pii/S0038071701001584>
- 546 Kyker-Snowman, E., Wieder, W. R., Frey, S. D., & Grandy, A. S. (2020). Stoichiometrically coupled carbon and  
547 nitrogen cycling in the Microbial-MIneral Carbon Stabilization model version 1.0 (MIMICS-CN v1. 0).  
548 *Geoscientific Model Development*, *13*(9), 4413-4434.
- 549 Lee, D., & Seung, H. S. (2000). Algorithms for non-negative matrix factorization. *Advances in neural information*  
550 *processing systems*, *13*.
- 551 Lei, J., Guo, X., Zeng, Y., Zhou, J., Gao, Q., & Yang, Y. (2021). Temporal changes in global soil respiration since  
552 1987. *Nature communications*, *12*(1), 403.
- 553 Liang, C., Amelung, W., Lehmann, J., & Kästner, M. (2019). Quantitative assessment of microbial necromass  
554 contribution to soil organic matter. *Global change biology*, *25*(11), 3578-3590.
- 555 Lugato, E., Lavalley, J. M., Haddix, M. L., Panagos, P., & Cotrufo, M. F. (2021). Different climate sensitivity of  
556 particulate and mineral-associated soil organic matter. *Nature Geoscience*, *14*(5), 295-300.
- 557 Marschner, B., & Kalbitz, K. (2003). Controls of bioavailability and biodegradability of dissolved organic matter in  
558 soils. *Geoderma*, *113*(3-4), 211-235.
- 559 Melillo, J. M., Frey, S. D., DeAngelis, K. M., Werner, W. J., Bernard, M. J., Bowles, F. P., et al. (2017). Long-term  
560 pattern and magnitude of soil carbon feedback to the climate system in a warming world. *Science*,  
561 *358*(6359), 101-105.
- 562 Nissan, A., Alcolombri, U., Peleg, N., Galili, N., Jimenez-Martinez, J., Molnar, P., & Holzner, M. (2023). Global  
563 warming accelerates soil heterotrophic respiration. *Nature communications*, *14*(1), 3452.
- 564 Raich, J. W., & Potter, C. S. (1995). Global patterns of carbon dioxide emissions from soils. *Global biogeochemical*  
565 *cycles*, *9*(1), 23-36.
- 566 Raich, J. W., Potter, C. S., & Bhagawati, D. (2002). Interannual variability in global soil respiration, 1980–94.  
567 *Global Change Biology*, *8*(8), 800-812.
- 568 Robertson, A. D., Paustian, K., Ogle, S., Wallenstein, M. D., Lugato, E., & Cotrufo, M. F. (2019). Unifying soil  
569 organic matter formation and persistence frameworks: the MEMS model. *Biogeosciences*, *16*(6), 1225-  
570 1248.
- 571 Rumpel, C., & Kögel-Knabner, I. (2011). Deep soil organic matter—a key but poorly understood component of  
572 terrestrial C cycle. *Plant and soil*, *338*, 143-158.
- 573 Sanderman, J., Baldock, J. A., Dangal, S. R. S., Ludwig, S., Potter, S., Rivard, C., & Savage, K. (2021). Soil organic  
574 carbon fractions in the Great Plains of the United States: an application of mid-infrared spectroscopy.  
575 *Biogeochemistry*, *156*(1), 97-114. <https://doi.org/10.1007/s10533-021-00755-1>
- 576 Scott, N. A., Cole, C. V., Elliott, E. T., & Huffman, S. A. (1996). Soil textural control on decomposition and soil  
577 organic matter dynamics. *Soil Science Society of America Journal*, *60*(4), 1102-1109.
- 578 Song, H.-S., Stegen, J. C., Graham, E. B., Lee, J.-Y., Garayburu-Caruso, V. A., Nelson, W. C., et al. (2020).  
579 Representing organic matter thermodynamics in biogeochemical reactions via substrate-explicit modeling.  
580 *Frontiers in microbiology*, *11*, 531756.
- 581 Sonnewald, M., Dutkiewicz, S., Hill, C., & Forget, G. (2020). Elucidating ecological complexity: Unsupervised  
582 learning determines global marine eco-provinces. *Science Advances*, *6*(22), eaay4740.  
583 <https://www.science.org/doi/abs/10.1126/sciadv.aay4740>
- 584 Sulman, B. N., Phillips, R. P., Oishi, A. C., Shevliakova, E., & Pacala, S. W. (2014). Microbe-driven turnover  
585 offsets mineral-mediated storage of soil carbon under elevated CO<sub>2</sub>. *Nature Climate Change*, *4*(12), 1099-  
586 1102.

- 587 Tfaily, M. M., Chu, R. K., Tolić, N., Roscioli, K. M., Anderton, C. R., Paša-Tolić, L., et al. (2015). Advanced  
588 solvent based methods for molecular characterization of soil organic matter by high-resolution mass  
589 spectrometry. *Analytical chemistry*, 87(10), 5206-5215.
- 590 Todd-Brown, K., Randerson, J., Hopkins, F., Arora, V., Hajima, T., Jones, C., et al. (2014). Changes in soil organic  
591 carbon storage predicted by Earth system models during the 21st century. *Biogeosciences*, 11(8), 2341-  
592 2356.
- 593 Turețcaia, A. B., Garayburu-Caruso, V. A., Kaufman, M. H., Danczak, R. E., Stegen, J. C., Chu, R. K., et al. (2023).  
594 Rethinking Aerobic Respiration in the Hyporheic Zone under Variation in Carbon and Nitrogen  
595 Stoichiometry. *Environmental Science & Technology*, 57(41), 15499-15510.  
596 <https://doi.org/10.1021/acs.est.3c04765>
- 597 Waring, B. G., Sulman, B. N., Reed, S., Smith, A. P., Averill, C., Creamer, C. A., et al. (2020). From pools to flow:  
598 The PROMISE framework for new insights on soil carbon cycling in a changing world. *Global Change*  
599 *Biology*, 26(12), 6631-6643.
- 600 Warner, D., Bond-Lamberty, B., Jian, J., Stell, E., & Vargas, R. (2019). Spatial predictions and associated  
601 uncertainty of annual soil respiration at the global scale. *Global Biogeochemical Cycles*, 33(12), 1733-  
602 1745.
- 603 Wieder, W. R., Hartman, M. D., Sulman, B. N., Wang, Y. P., Koven, C. D., & Bonan, G. B. (2018). Carbon cycle  
604 confidence and uncertainty: Exploring variation among soil biogeochemical models. *Global change*  
605 *biology*, 24(4), 1563-1579.
- 606 Witzgall, K., Vidal, A., Schubert, D. I., Höschen, C., Schweizer, S. A., Buegger, F., et al. (2021). Particulate organic  
607 matter as a functional soil component for persistent soil organic carbon. *Nature Communications*, 12(1),  
608 4115.
- 609
- 610

611

612

*Geophysical Research Letters*

613

Supporting Information for

614

**Supporting Information of**

615

**Scaling High-resolution Soil Organic Matter Composition to Improve Predictions of**

616

**Potential Soil Respiration Across the Continental United States**

617

Cheng Shi<sup>a</sup>, Maruti Mudunuru<sup>b</sup>, Maggie Bowman<sup>c</sup>, Qian Zhao<sup>c</sup>, Jason Toyoda<sup>c</sup>, Will Kew<sup>c</sup>, Yuri

618

Corilo<sup>c</sup>, Odeta Qafoku<sup>c</sup>, John R. Bargar<sup>c</sup>, Satish Karra<sup>c</sup>, & Emily B. Graham<sup>d,e\*</sup>

619

<sup>a</sup>Oregon State University, Department of Biological & Ecological Engineering, Corvallis, OR, United States.

620

<sup>b</sup>Energy and Environment Directorate, Pacific Northwest National Laboratory, Richland, WA, United States.

621

<sup>c</sup>Environmental Molecular Science Laboratory, Pacific Northwest National Laboratory, Richland, WA,

622

United States.

623

<sup>d</sup>Earth and Biological Sciences Directorate, Pacific Northwest National Laboratory, Richland, WA, United

624

States.

625

<sup>e</sup>School of Biological Sciences, Washington State University, Pullman, WA, United States.

626

627 \*Corresponding author: emily.graham@pnnl.gov

628

629

630 **Contents of this file**

631

Text S1 to S5

632

Figures S1 to S10

633

Tables S1 to S3

634

635

636

637

638

639 **Introduction**

640 The supporting information includes extended methods (Text S1, Text S2, and Text S3),  
641 and extended interpretation of results (Text S4 and Text S5). The extended methods sections  
642 provide extra details of analytical methods, data processing methods, and justifications. The  
643 extended results summarize the holistic relationships between soil physicochemistry, potential  
644 soil respiration, and SOM composition. The supporting figures (Figure S1 to S10) and supporting  
645 tables (Table S1 to S3) are used in the main manuscript and supporting text to report detailed  
646 findings. All the data used in this study is publicly available on Zenodo at  
647 <https://zenodo.org/records/10888508>.

#### 648 **Text S1.** Soil physicochemistry and SOM composition analysis

649 Per the methods outlined by Bowman et al. (2023), we divided the 30-cm cores collected  
650 from the fields into three 10-cm intervals, where only the top 10-cm (hereafter, surface or  
651 surficial soil) and bottom 10-cm (hereafter, subsoil) sections were used for further analysis. We  
652 mixed the top sections with three short cores (10-cm cores sampled at the same site) to  
653 homogenize the local variation. The soils were then sieved through 4 mm sieves separately to  
654 remove rocks and root structures. We measured gravimetric water content (GWC) by drying 10 g  
655 of soil for 24 hours in a drying oven at 100 °C. We measured soil pH by mixing 20 g of dry soil  
656 with 20 mL of DI water (1000 rpm on reciprocating shaker for 15 minutes) and testing with a  
657 calibrated pH probe. Soil microbial biomass C and nitrogen (N) content were measured via  
658 chloroform fumigation (Brookes et al., 1985; Witt et al., 2000; Zhao et al., 2022). We extracted  
659 phosphorus contents using Bray (pH < 7) or Olsen extractions (pH > 7) (Bray & Kurtz, 1945;  
660 Corbridge, 1980), and extracted nitrate and ammonium with 0.5M K<sub>2</sub>SO<sub>4</sub> and tested by  
661 colorimetric methods. Ion concentrations of potassium (K), calcium (Ca), magnesium (Mg), and  
662 sodium (Na) from 1:10 ammonium acetate extraction, Zinc (Zn), manganese (Mn), copper (Cu),  
663 iron (Fe), boron (B), and sulfate (SO<sub>4</sub><sup>2-</sup>) from 1:2 soil to diethylenetriaminepentaacetic acid  
664 (DPTA) extraction were measured using Inductively coupled plasma mass spectrometry (ICP-  
665 MS). We measured total C and N using the AOAC official methods 972.43 (AOAC, 2006). Soil  
666 texture was measured by hydrometer analysis. Finally, we assessed potential soil respiration  
667 using the CO<sub>2</sub> burst method with 24 hours of incubation at 24 °C (Bowman et al., 2023).

668 We extracted water-soluble SOM by mixing 6 g of dry soil with 30 ml DI water in  
669 triplicates, shaken for 2 hours at 800 rpm, and centrifuged at 6,000 rpm for 8 minutes. 5 ml of  
670 supernatant was acidified with 2 µl concentrated phosphoric acid (37%), and then loaded onto  
671 Agilent Bond Elut PPL solid phase extraction cartridges (Dittmar et al., 2008) with Gilson ASPEC®  
672 SPE system. A Bruker 7-T Fourier transform ion cyclotron resonance mass spectrometry (FTICR  
673 MS) at the Environmental Molecular Sciences Laboratory (EMSL) in Richland, WA, was used to  
674 analyze SOM composition, with a negative ionization mode and ion accumulation time at 0.01  
675 or 0.025 seconds (depending on dissolved organic C concentration). The measured mass  
676 accuracy was typically within 1 ppm. One lab blank and one Suwannee River Fulvic Acid (SRFA)  
677 sample (20 ppm) were tested every 30 soils to evaluate instrument performance.

678 We used CoreMS (<https://github.com/EMSL-Computing/CoreMS>) to process raw FTICR  
679 MS data in Python. Noise thresholding was performed with signal-to-noise threshold (5 std.),

680 mass error (0.3 ppm), and stoichiometric limits from domain knowledge (C: 1-90, H: 4-200, O:1-  
681 23, N: 0-3, S: 0-2, P: 0-1). Suwannee River fulvic acid (SRFA) standards were used to set a  
682 calibration threshold for all soils in the same batch. Molecular formula was assigned based on  
683 both accurate mass and filtered by their confidence score from CoreMS. After calibration and  
684 formulae assignment, we filtered the assigned peaks by  $m/z$  between 200 to 1,000, present in at  
685 least 2 out of 3 replicates, not present in two or more lab blanks, and with formulae confidence  
686 scores (combines  $m/z$  error and isotopic pattern) above 0.7 (Corilo et al., 2021).

687

### 688 **Text S2.** NMF $k$ model assumption and model selection

689 We used NMF $k$  to decompose the SOM composition matrix into multiple basis  
690 signatures, due to its ability to capture unique and sparse patterns from complex data (D. Lee &  
691 Seung, 2000). The underlying assumption of NMF $k$  is that there are similar distributions of  
692 variables (SOM formula in this study) across samples, such that the main characteristics of each  
693 sample can be represented by the combination of a limited number of non-negative basis  
694 components (signatures) (Paatero & Tapper, 1994). It has also been widely used in  
695 environmental forensics (Johnson et al., 2015; Rodenburg et al., 2011), text mining (Pauca et al.,  
696 2004), and face recognition (Guillamet & Vitria, 2002). For example, Vesselinov et al. (2018) used  
697 NMF $k$  to identify unknown sources of groundwater recharge driven by various physical and  
698 chemical processes; while Cai et al. (2017) used NMF to extract key features and reveal temporal  
699 patterns in microbial communities. Instead of relying on linear data transformations like  
700 principal components analysis (PCA), NMF $k$  uses non-negativity constraints that makes it better  
701 suited to identify representative SOM signatures and evaluate their distribution in diverse  
702 samples. Furthermore, the additive fashion of extracted signatures to represent SOM  
703 composition by NMF $k$  fit the intuition of different pools of SOM molecules adding up to the  
704 combined mixture of SOM in a certain sample. Therefore, the NMF $k$  extracted SOM signatures  
705 are more explainable compared to PCA or other ordination techniques.

706 The number of signatures ( $k$ ) was determined by  $k$ -means clustering coupled to a  
707 silhouette coefficient with a threshold of 0.5 to evaluate model stability (Bhattarai et al., 2020;  
708 Vangara et al., 2021). We evaluated a range of  $k$  from 2 to 20 for both models (surface soil and  
709 subsoil), where the highest  $k$ -model above the threshold ( $> 0.5$ ) is selected as the final model.  
710 This is because the selected model should have good separation (more separation with a larger  
711  $k$ ) between different non-negative signatures but also a stable solution (above the threshold of  
712 silhouette coefficient) at the same time. To visualize the composition of each NMF $k$  signatures  
713 ( $W$ -matrix), we generated a heatmap of SOM formula with normalized weights (0-1)  $>0.5$  in at  
714 least one NMF $k$ , clustered by van Krevelen class assignment (clustermap function from seaborn  
715 package). Within each inferred chemical class of SOM formula, we further clustered formula  
716 using the "linkage" method from the *scipy* package ("ward" method with "Euclidean" distance) to  
717 illustrate the difference between NMF $k$  signatures.

### 718 **Text S3.** Gradient boosting regression model development

719 Gradient boosting is a machine learning algorithm that combines multiple weak models,  
720 such as decision trees, iteratively into a stronger model, where each weak model learns from the



721 residual error from the previous model (Friedman, 2001). It is one of the most powerful and  
722 effective machine learning models that is widely used in many different areas. Using an  
723 ensemble method, gradient boosting regression is capable to generate predictions from  
724 multiple decision tree models and thus provide a more robust prediction. It usually has better  
725 performance with smaller dataset, because it is less likely to overfit the data (Hastie et al., 2009).  
726 Therefore, it is suitable for predicting soil respiration with physicochemistry and NMFk extracted  
727 SOM signatures.

728 We performed feature selection on physicochemical factors by statistical relevance (Table  
729 S1) to remove irrelevant features that likely introduce noises and leads to overfitting (Christ et  
730 al., 2018; Yuan et al., 2019). *stats.linregress* function from *scipy* package (v 1.11.4) in Python (v  
731 3.7.1) was applied to calculate the fitted line,  $r^2$  value (*rvalue*<sup>2</sup>, Pearson correlation), and p-value  
732 (*pvalue*). Pairwise plots with regression fitting were generated by the *pairplot* function from the  
733 *seaborn* package (v 0.12.1) in Python. Total C, total N, CEC, Mn and soil moisture were selected  
734 as predictors for surface soil models. Total C, total N, total base, CEC, Mg and soil moisture were  
735 selected for subsoil models.

736 Model hyperparameters were tuned first with 5-fold cross validation on 80% of soils in  
737 each dataset (*train\_test\_split* in scikit-learn, with the same *random\_state* for models in the same  
738 layer) using *RandomizedSearchCV* function from scikit-learn. We then used the best-tuned  
739 parameters with 80% of soils to build the finalized model. Root means square error (RMSE) was  
740 used to evaluate the error of models. Detailed settings of the hyperparameter dictionary for  
741 *RandomizedSearchCV* and the best-tuned parameter set used for the final model are shown in  
742 Table S3. All the models were then tested with the other 20% of soils to compare their  
743 performance. The feature importance of each predictor was determined using MDI importance  
744 (mean decrease in impurity) to infer potential relationships between soil physicochemistry, SOM  
745 composition, and potential soil respiration. Partial dependence plots were used to evaluate the  
746 sensitivity of potential respiration in response to selected predictors.

747 To avoid the impacts of the increased number of predictors on improved model  
748 performance for surface soils (physicochemistry model:  $n = 5$ , SOM model:  $n = 7$ ), we developed  
749 another version of SOM model without the two least important predictors (NMF7, NMF4). The  
750 model performance was still better (testing  $R^2 = 0.48$  vs.  $0.44$ ) compared to the physicochemistry  
751 model with the same number of predictors ( $n = 5$ ).

752

#### 753 **Text S4.** Soil respiration and physicochemistry

754 Soil moisture, total C, and total N appeared to regulate soil respiration in both surface  
755 soil and subsoil, as evidenced by positive correlations of total C, N, and moisture with potential  
756 soil respiration (Figure S4). This is consistent with previous work describing relationships  
757 between these properties and soil respiration, as well as other factors that we observed to be  
758 correlated with respiration including pH and CEC (Chen et al., 2014; K.-H. Lee & Jose, 2003; Riaz  
759 & Marschner, 2020; Waring et al., 2020). Soil physical properties (e.g, moisture and pore space

760 connectivity) can constrain microbial access to SOM molecules and nutrients isolated in soil pore  
761 networks, thereby regulating microbial respiration of SOM (Falloon et al., 2011; Moyano et al.,  
762 2013; Orchard & Cook, 1983; Waring et al., 2020; Xu et al., 2004). Additionally, C and N can limit  
763 soil respiration through stoichiometric constraints on biomass production (Elser et al., 2000;  
764 Graham & Hofmockel, 2022; Soong et al., 2020; Wang & Houlton, 2009). Notably, field  
765 temperature was not correlated with potential soil respiration in this study (Figure S4h). We  
766 posit this lack of relationship is due to the standardization of potential soil respiration assays, in  
767 which all respiration rates were measured at a common temperature. Future work to extend the  
768 methods applied here to field-based estimates of microbial respiration is a promising avenue to  
769 further constrain microbial respiratory pathways relevant to soil carbon cycling.

770 We propose that differences in potential respiration between surface and subsoil may be  
771 related to variation in soil C composition and stabilization mechanisms across soil layers. We  
772 observed a steeper correlation between total C and potential soil respiration in surface soils than  
773 in subsoils (Figure S4), despite similar slopes for relationships of N and moisture with respiration  
774 at both depths. While we anticipated that microbial respiration would decrease significantly with  
775 soil depth (Changming Fang & John B. Moncrieff, 2005), the change in the nature of the  
776 relationship between C and respiration suggests that differences in SOM composition or  
777 microbial access to C substrates could be associated with potential rates of respiration. Surface  
778 soils are generally rich in relatively bioavailable water-extractable organic matter and contain  
779 higher proportions of microbial biomass in contrast to subsoils that are more mineral with lower  
780 pore space connectivity and larger pools of mineral-associated organic matter (Schimel, 2021).  
781 Given previously observed differences in SOM composition and soil structure, we hypothesize  
782 that factors including oxygen availability and alternative electron acceptors may influence  
783 heterotrophic respiration to a greater degree than soil C as depth increases.

784 We also found a suite of correlations between elements and potential soil respiration  
785 that may reflect the influence of vegetation across rooting profiles; however, associations  
786 between inorganic nutrients ( $\text{NH}_4^+$ ,  $\text{NO}_3^-$ ,  $\text{PO}_4^{3-}$ ) and respiration were conspicuously absent  
787 ( $p > 0.05$ , Table S1) (Fan et al., 2022; Mori et al., 2018; Nicolás et al., 2019; Subedi et al., 2021). Mg,  
788 Mn, Zn, and sulfate were correlated to potential soil respiration and are known to have strong  
789 impacts on plant productivity that provides chemically labile C sources for microbial respiration  
790 (Chao et al., 2019; Gransee & Führs, 2013; Opfergelt et al., 2017). Mn can also influence soil  
791 respiration by regulating the activities of Mn peroxidase enzyme, a lignin-degrading enzyme  
792 produced by fungi and *Actinobacteria* (Kranabetter et al., 2021; Li et al., 2021; Neupane et al.,  
793 2023; Santos & Herndon, 2023; Whalen, 2017). Because total N corresponded to potential soil  
794 respiration, the lack of relationship between respiration and inorganic nutrients may indicate  
795 organic nutrients as key drivers of soil respiration. Alternatively, inorganic nutrient limitations  
796 that vary tremendously through space and time may not be observable across different  
797 ecosystems at the continental scale (Taylor & Townsend, 2010; M. Zhang et al., 2021).

798 In addition to patterns in soil physicochemistry, we observed geographic patterns in  
799 potential soil respiration that contrasted with some previous estimates (Nissan et al., 2023),  
800 including high rates of potential soil respiration in the midwestern and mid-Atlantic regions, and

801 at high elevations (Figure S5). A notable difference between Nissan et al. and the current study is  
802 that Nissan et al. report simulated mean annual values of heterotrophic respiration in soils, while  
803 the current study reports the measured potential respiration rates of sieved soils collected  
804 during the summer months. Because high latitude and high elevation ecosystems can exhibit  
805 intense, short-lived peaks of biomass during summertime (Siles et al., 2017), soils collected  
806 during this period may have relatively extreme rates of potential respiration that are averaged  
807 out at the annual scale. Another interpretation for higher potential soil respiration at high  
808 elevation is that relative humidity typically increases with elevation and thus can stimulate  
809 higher microbial activities and SOM decomposition (Berryman et al., 2014). In contrast,  
810 comparatively low potential soil respiration recorded in the Southeastern United States could  
811 also reflect the comparatively low C content of these soils that has been associated with faster  
812 turnover rates and high year-round temperatures (Brye et al., 2016).

813

#### 814 **Text S5.** SOM composition and relationship with potential soil respiration

815 Differences in SOM composition with soil depth and across the continental United States  
816 were associated with potential soil respiration, supporting previous studies showing  
817 relationships between SOM composition and soil respiration rates (Figure S5). (Bond-Lamberty &  
818 Thomson, 2010; Curiel Yuste et al., 2007; Changming Fang & John B Moncrieff, 2005) Regardless  
819 of depth or geographic location, the diversity of water-extractable SOM compounds appeared  
820 to be a common factor in regulating potential soil respiration — soils with higher potential  
821 respiration generally had more diverse pools of water-extractable SOM (Figure S5e-f).

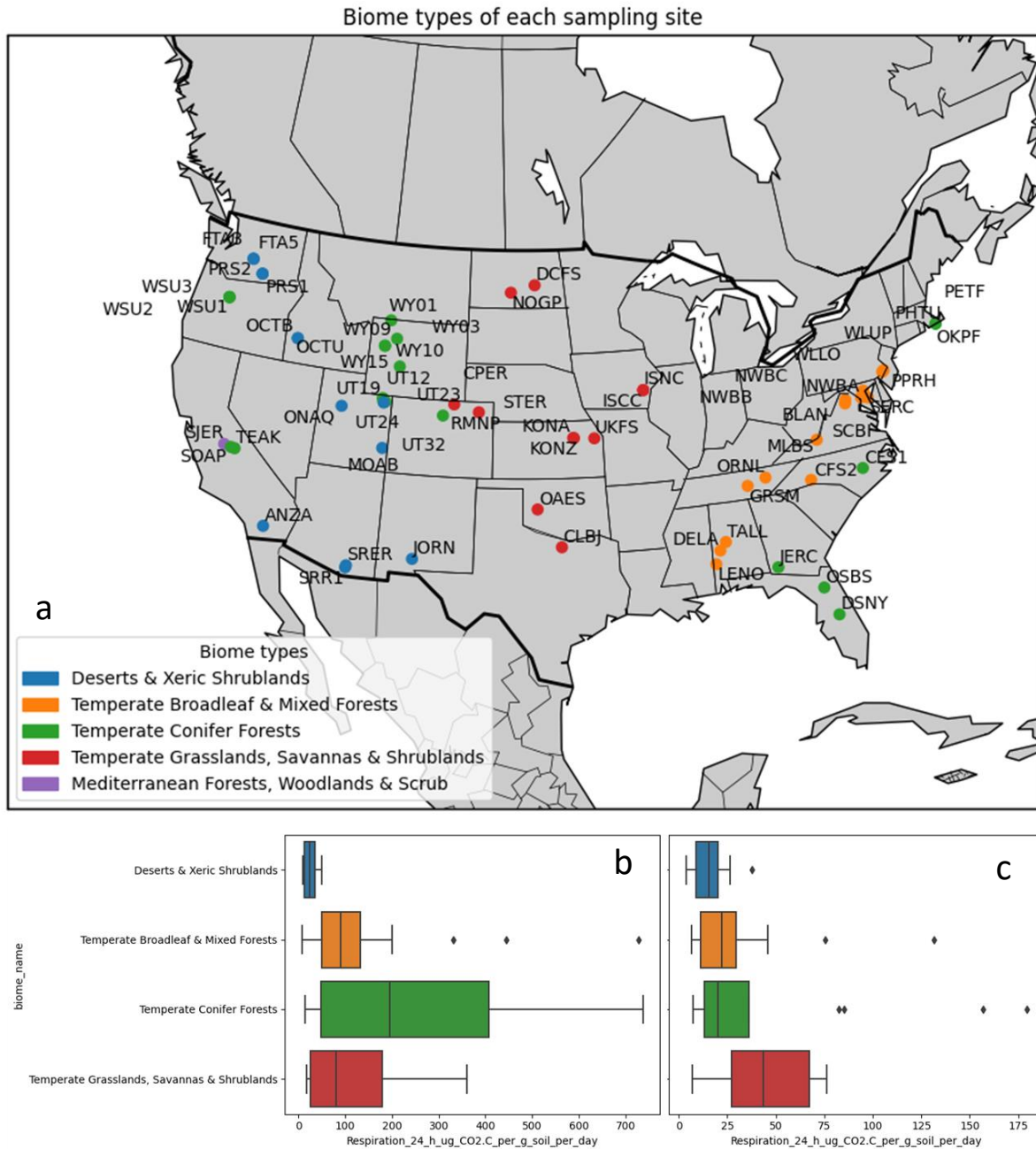
822 For surface soils, NMF3 presented as the largest relative contributor to SOM composition  
823 in 20 soils across all biomes (i.e., highest weighting in H-matrix, hereafter, 'dominant signature',  
824 Figure S6). NMF2, NMF5, and NMF7 served as the dominant signature in at least 9 soils each.  
825 For subsoils, NMF5 and NMF2 were the dominant signature in 27 soils and 16 soils respectively  
826 distributed across all biomes in the continental United States. There was no single NMF  
827 signature that could exclusively represent SOM composition of all sites in the same region for  
828 either surface or subsoils, suggesting that SOM composition at local sites is best summarized by  
829 a combination of multiple NMFs.

830 Our results were consistent with a paradigm in which chemically bioavailable, plant-  
831 derived molecules including proteins and amino sugars are degraded through soil profiles and  
832 transformed into microbially-derived byproducts that are stabilized via organo-mineral  
833 associations (Kallenbach et al., 2016; Roth et al., 2019; Zhao et al., 2020); whereas more  
834 chemically recalcitrant compounds (e.g., lignins and tannin) are preserved due to their lower  
835 thermodynamic bioavailability (Kögel-Knabner, 2002; Kramer & Gleixner, 2008; Rumpel & Kögel-  
836 Knabner, 2011). Coincident decreases in SOM diversity from surface to subsoils were also  
837 associated with decreases in potential soil respiration (Figure S5d), further supporting a link  
838 between SOM pool composition and microbial decomposition. (Davenport et al., 2023; Kramer &  
839 Gleixner, 2008) The comparatively diverse SOM pools in surface soils contained more  
840 bioavailable compounds than subsoils, including protein-, amino sugar-, and lipid-like

841 compounds.(Jones, 1999; Marschner & Kalbitz, 2003) The number of formulae in these chemical  
842 classes declined with depth, and formula that were common to both soil layers primarily  
843 included chemical classes with low putative bioavailability such as lignin-, tannin-, and  
844 condensed hydrocarbon-like compounds (Marschner & Kalbitz, 2003).

845         There was a weak correlation between SOM composition and potential respiration in  
846 subsoils. NMF4 (associated with high-respiration soils) and NMF5 (associated with low-  
847 respiration soils) had the largest disparities in weighting across subsoils (Figure 2e). Consistent  
848 with observations from surface soils, subsoil NMF4 contained the largest proportion of amino  
849 sugar- and protein-like formula compared to other subsoil NMFs, while NMF5 was almost  
850 entirely composed of lignin- and tannin-like compounds (Marschner & Kalbitz, 2003). The  
851 composition of water-extractable SOM in mineral subsoils is an emerging area of research, and  
852 it remains unclear how different SOM chemistries contribute to subsoil respiration (Rumpel &  
853 Kögel-Knabner, 2011). Our results suggest some consistencies in the chemical mechanisms of  
854 SOM bioavailability across soil horizons. However, one subsoil NMF (NMF2) had unexpectedly  
855 large weightings in high respiration subsoils despite low bioavailability typically associated with  
856 its chemical constituents (Lehmann et al., 2020; Marschner & Kalbitz, 2003). The remaining  
857 subsoil NMFs (1 and 3) were present in both low- and high-respiration subsoils. This denotes  
858 that factors beyond chemical recalcitrance or beyond the most commonly measured (water-  
859 extractable) SOM pool are critical to understanding belowground C cycling (Angst et al., 2021; H.  
860 Zhang et al., 2020).

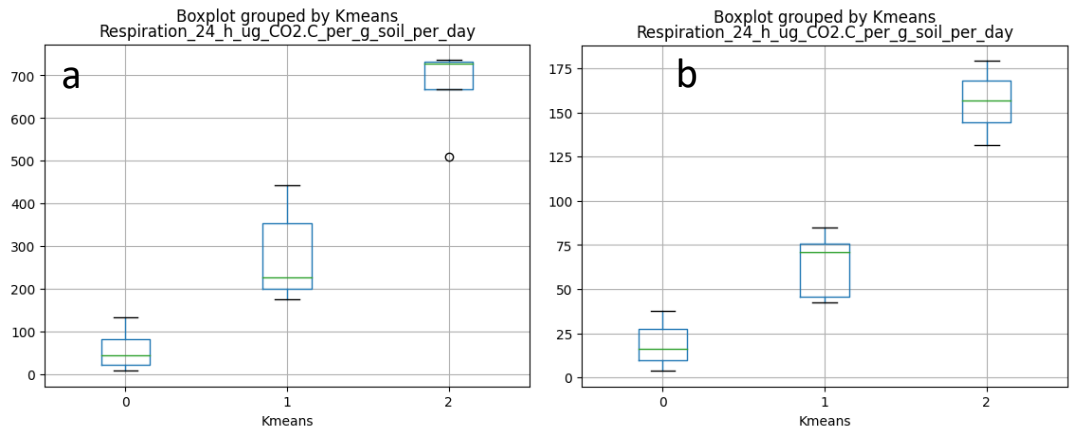
861



862  
863  
864  
865

**Figure S1.** Sampling locations, sample names, and their biome types obtained from WWF terrestrial ecoregions (a). Difference of soil potential respiration by biomes in b) surface and c) subsurface.

866

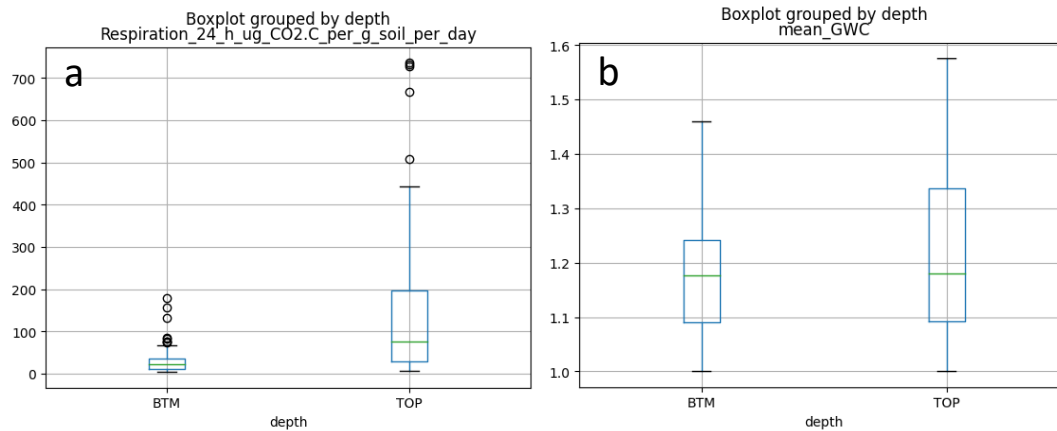


867

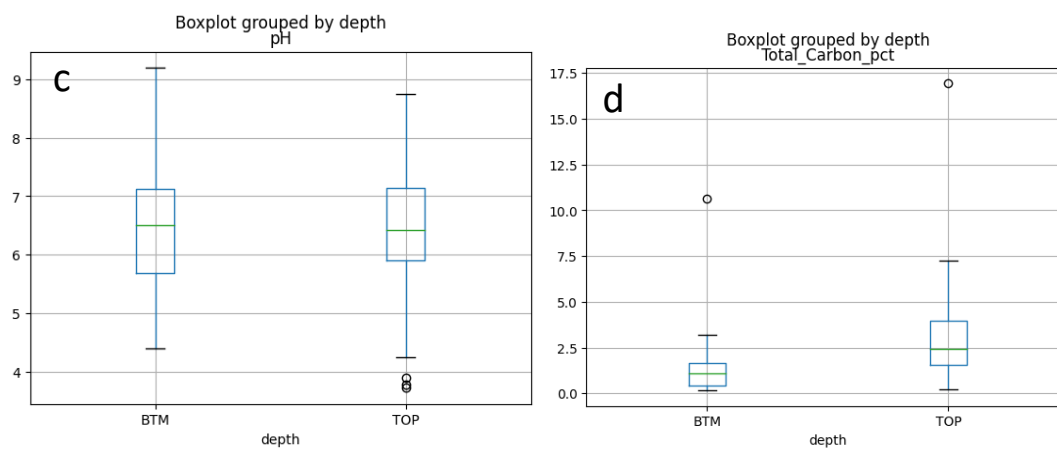
868 **Figure S2.** k-means clustering of potential soil respiration rates in a) surface soils and b)  
869 subsoils.

870

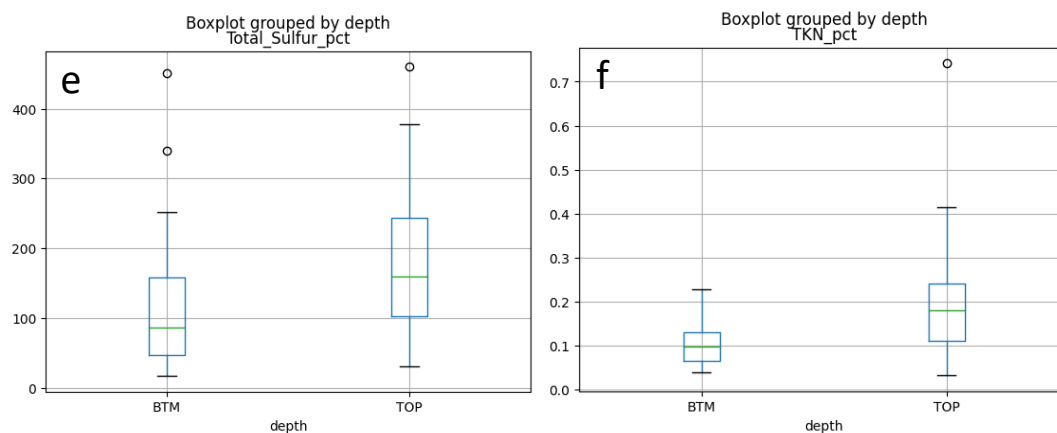
871



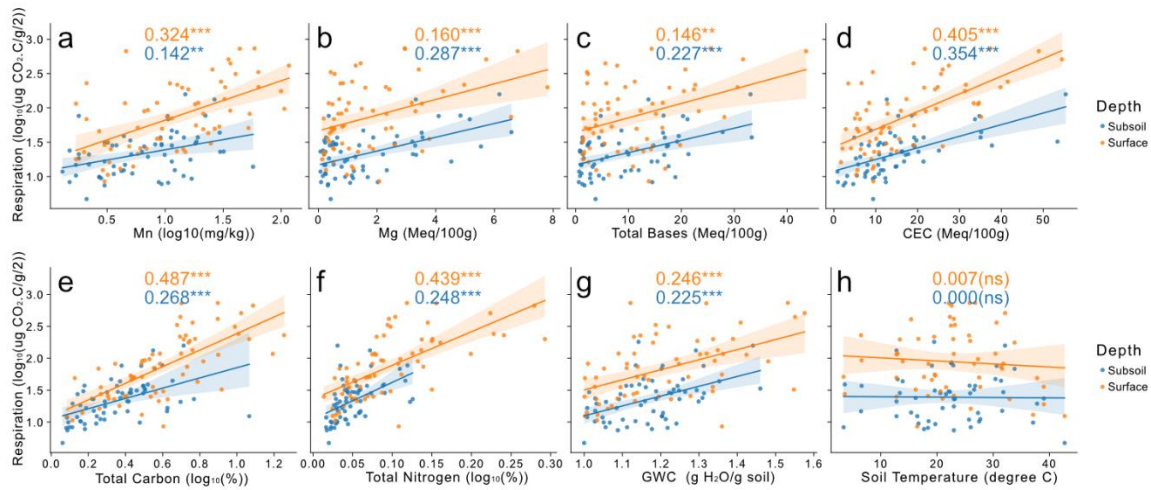
872



873



874 **Figure S3.** Boxplots of selected soil physicochemical variables between surface and subsoils. a)  
 875 potential respiration, b) moisture content, c) pH, d) total C, e) total S, f) total N. TOP: surface  
 876 soils, BTM: subsoils.



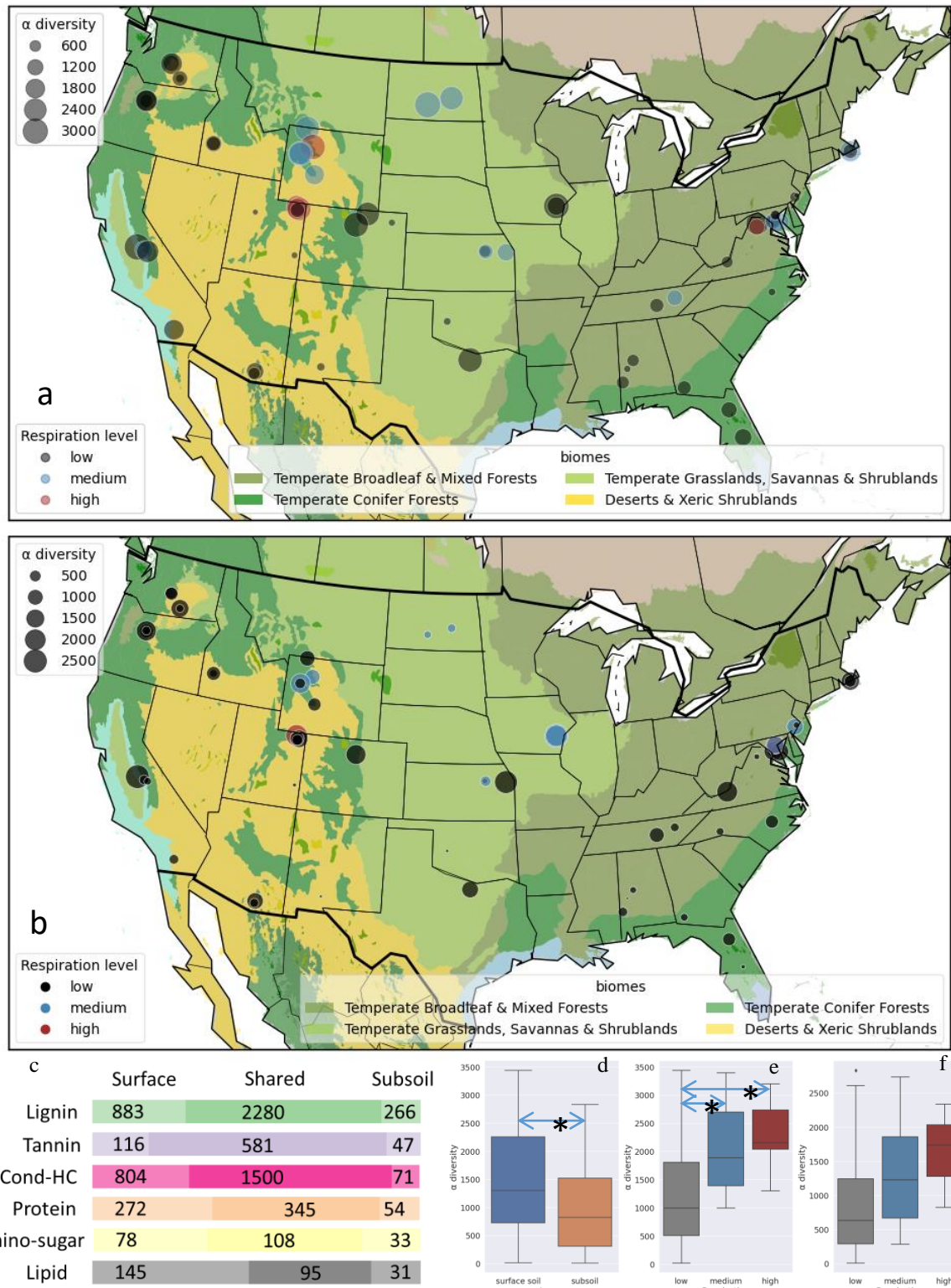
877

878

879 **Figure S4.** The relationship between soil characteristics and potential respiration. (a-h) show  
 880 [Manganese (Mn), Magnesium (Mg), Total Bases, CEC, Total C, Total N, GWC, Soil Temperature],  
 881 respectively. Orange represents surface soils and blue represents subsoils. Lines denote the  
 882 fitted linear regression function. Numbers on each panel are R<sup>2</sup> value from linear regression, the  
 883 stars behind represents statistical significance (\*\*\* (p ≤ 0.001), \*\* (p ≤ 0.01), ns (p > 0.05)).

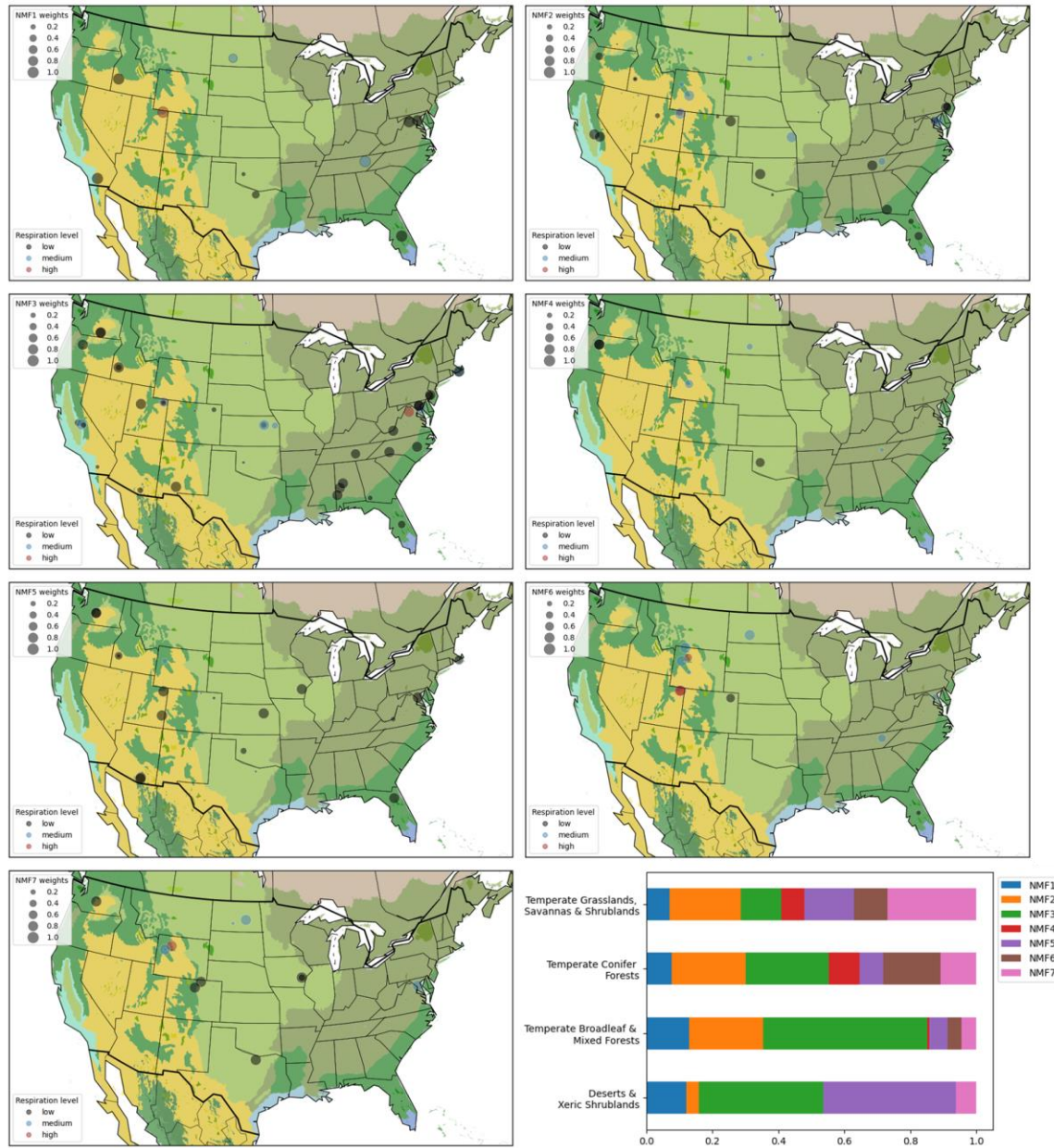
884





885 **Figure S5.** Spatial distribution of soil respiration levels (labeled by colors) and alpha diversity of  
 886 SOM pools in each sample (bubble sizes) of a) surface soils and b) subsoils. Soil respiration  
 887 levels are determined by k-means clustering on potential soil respiration rates (Figure S2). Soils

888 from temperate conifer forests and temperate grasslands, savannas & shrublands have relatively  
889 higher respiration rates compared to other biomes (Figure S1). (c) The number of shared and  
890 unique SOM compounds identified between surface and subsoils, grouped by van Krevelen  
891 classification. (d) Alpha diversity of SOM in surface vs. subsoil soils ( $p < 0.05$  from ANOVA, \*:  
892  $p < 0.05$  from Tukey's HSD test) (e) Alpha diversity of SOM in surface soils across different levels  
893 of potential respiration ( $p < 0.05$  from ANOVA, \*:  $p < 0.05$  from Tukey's HSD test) (f) Alpha  
894 diversity of SOM in subsoils across different levels of potential respiration ( $p < 0.05$  from  
895 ANOVA)  
896



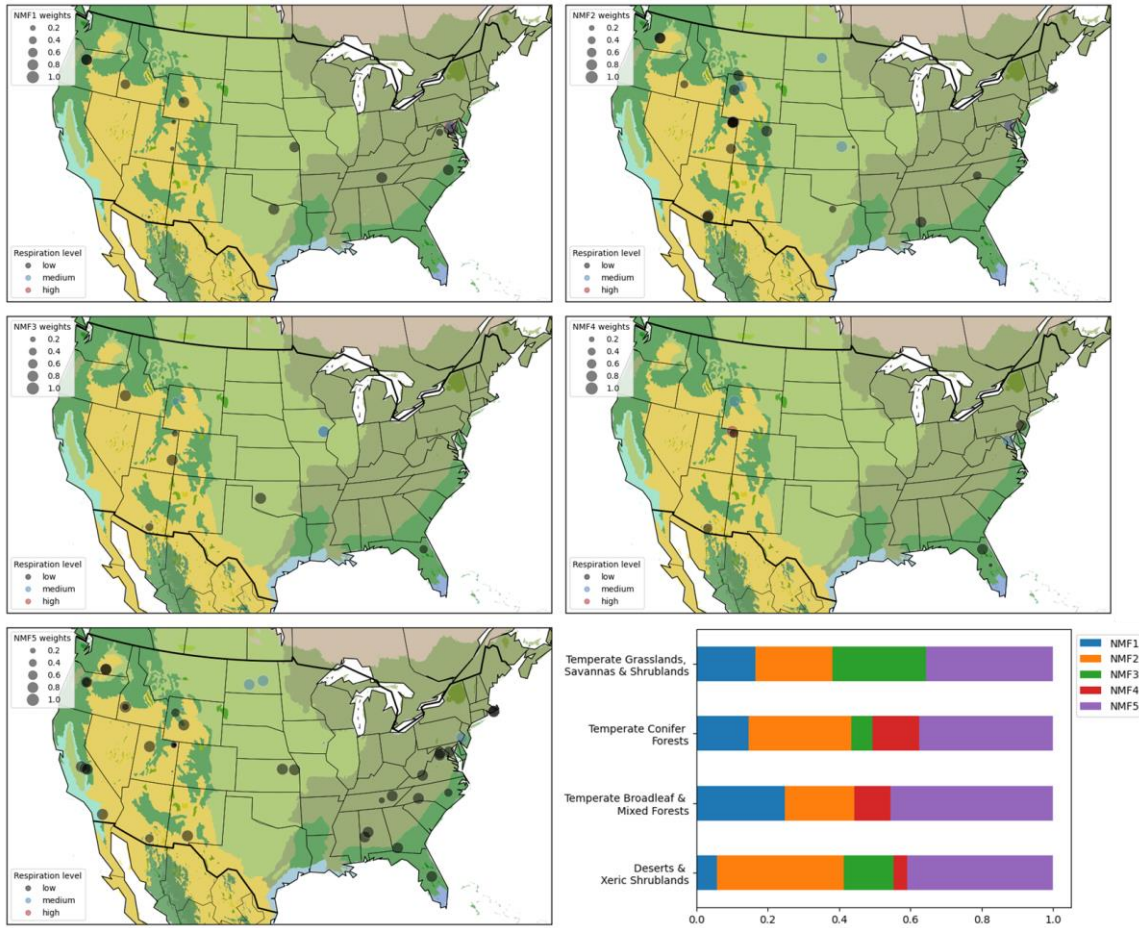
**Figure**

897 **S6.** Normalized weights for each surface soil NKfK (i.e., NMF1-7) are shown sequentially in each  
 898 map (one map per NMF). Weights are shown by bubble size, and bubbles are colored by  
 899 respiration level. The relative contribution of the 7 types in each biome is shown by the stacked  
 900 bar char. Deserts & Xeric Shrublands (N = 13), Temperate Broadleaf & Mixed Forests (N = 17),  
 901 Temperate Conifer Forests (N = 21), Temperate Grasslands, Savannas & Shrublands (N = 11).  
 902

903

904

905



906  
 907  
 908  
 909  
 910  
 911  
 912

**Figure S7.** Normalized weights for each subsoil NKfK (i.e., NMF1-5) are shown sequentially in each map (one map per NMF). Weights are shown by bubble size, and bubbles are colored by respiration level. The relative contribution of the 5 types in each biome is shown by the stacked bar chart. Deserts & Xeric Shrublands (N = 13), Temperate Broadleaf & Mixed Forests (N = 17), Temperate Conifer Forests (N = 21), Temperate Grasslands, Savannas & Shrublands (N = 9).

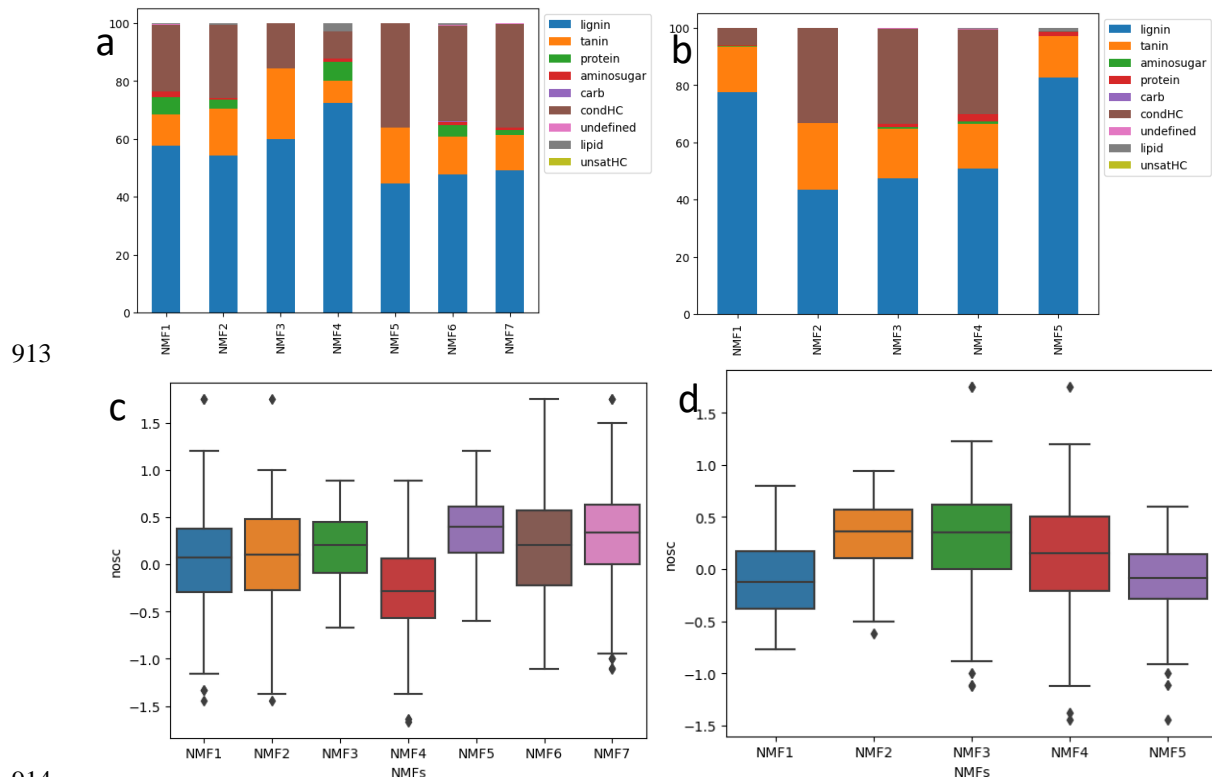


**Figure S8.** Relative contribution of each compound class to each NMFk in a) surface soil and b) subsoil. Boxplot shows the difference of Nominal Oxidation State of Carbon (NOSC) values for each NMF in c) surface soil and d) subsoil. Only features with normalized weights of greater than 0.5 are included in Figure S8.

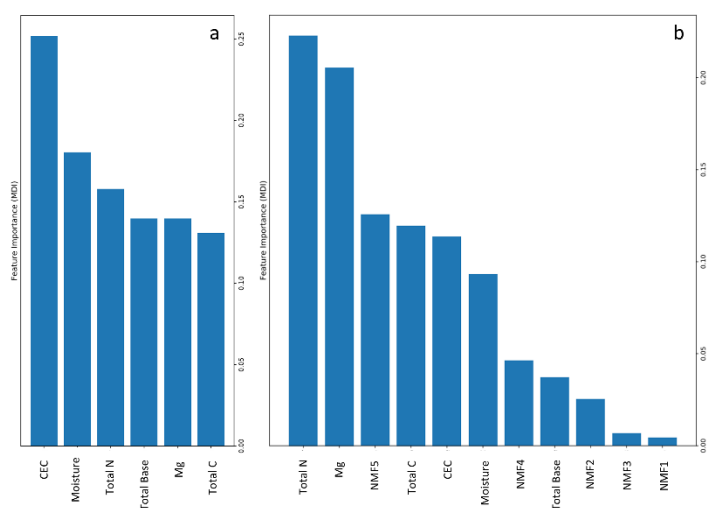
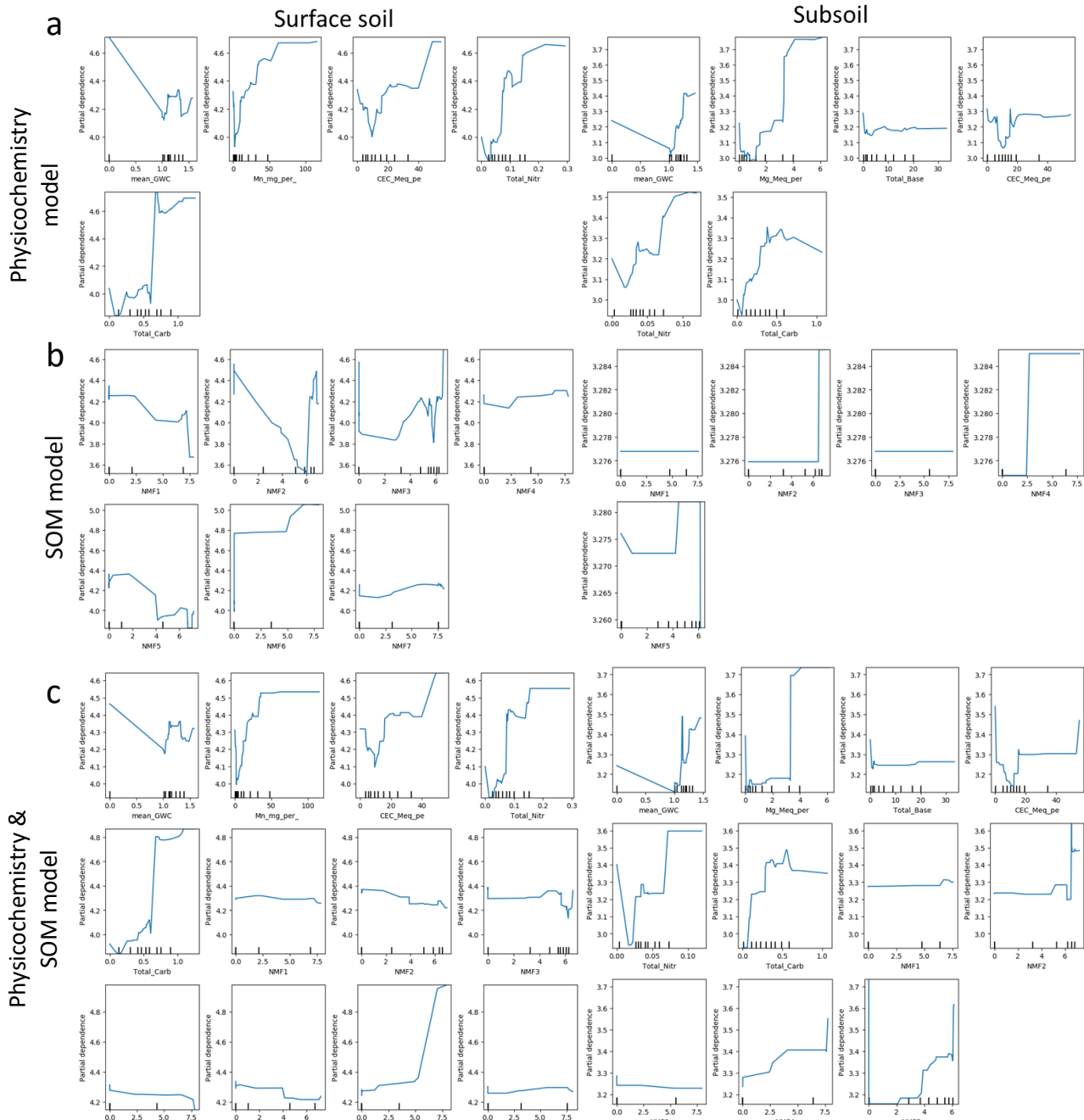


**Figure S9.** Relative importance of each predictor in subsoil potential respiration models. a) Physicochemistry Model, with physicochemical variables only. b) Physicochemistry & SOM model with both physicochemical variables and SOM types. (The SOM model for subsoil did not yield adequate performance (Table 1) and therefore is not reported here).



925

926

927 **Figure S1.** Partial dependence of potential respiration to predictors of soil physicochemistry  
 928 and/or SOM composition in surface and subsoil models. a) Physicochemistry model with  
 929 physicochemical variables for surface soil (left) and subsoil (right). b) SOM model with SOM  
 930 variables for surface soil (left) and subsoil (right, low performance), c) Physicochemistry & SOM  
 931 model with both physicochemical and SOM variables for surface soil (left) and subsoil (right).

		Surface	Surface	Subsoil	Subsoil
		R <sup>2</sup>	p-value	R <sup>2</sup>	p-value
935	Mn	<b>0.324</b>	<b>0.000</b>	<b>0.142</b>	<b>0.003</b>
936	Mg	<b>0.160</b>	<b>0.001</b>	<b>0.287</b>	<b>0.000</b>
937	K	0.004	0.638	0.053	0.071
938	Na	0.005	0.577	0.026	0.211
939	B	<b>0.119</b>	<b>0.006</b>	0.018	0.295
940	Zn	<b>0.173</b>	<b>0.001</b>	<b>0.102</b>	<b>0.011</b>
941	Fe	<b>0.089</b>	<b>0.017</b>	0.043	0.106
942	Cu	<b>0.092</b>	<b>0.016</b>	<b>0.133</b>	<b>0.004</b>
943	Total Base	<b>0.146</b>	<b>0.002</b>	<b>0.227</b>	<b>0.000</b>
944	CEC	<b>0.405</b>	<b>0.000</b>	<b>0.354</b>	<b>0.000</b>
945	Total C	<b>0.487</b>	<b>0.000</b>	<b>0.268</b>	<b>0.000</b>
946	Total N	<b>0.439</b>	<b>0.000</b>	<b>0.248</b>	<b>0.000</b>
947	Total S	<b>0.080</b>	<b>0.028</b>	0.036	0.160
948	GWC	<b>0.246</b>	<b>0.000</b>	<b>0.225</b>	<b>0.000</b>
949	Soil T	0.007	0.545	0.000	0.919
950	pH	<b>0.116</b>	<b>0.004</b>	0.007	0.513
951	SO4	<b>0.172</b>	<b>0.001</b>	0.002	0.759
952	P	0.001	0.855	0.003	0.695
953	NH4	0.002	0.761	0.000	0.992
954	NO3	0.004	0.634	0.004	0.634
955	Sand%	<b>0.140</b>	<b>0.001</b>	<b>0.176</b>	<b>0.000</b>
956	Silt%	<b>0.081</b>	<b>0.017</b>	<b>0.077</b>	<b>0.022</b>
957	Clay%	<b>0.157</b>	<b>0.001</b>	<b>0.182</b>	<b>0.000</b>
958	Elevation	<b>0.136</b>	<b>0.006</b>	<b>0.090</b>	<b>0.029</b>
959	alpha_div	<b>0.159</b>	<b>0.001</b>	<b>0.143</b>	<b>0.003</b>

960 **Table S1.** Coefficient of Determination between potential soil respiration and soil  
 961 physicochemistry (Pearson's correlation R-square). The bold texts highlight significant  
 962 relationships with p-value <0.05.

963

964

	Physicochemistry Model	SOM Model	Physicochemistry & SOM Model
Surface_CV (RMSE)	0.80	1.05	0.82
Surface_test (RMSE)	0.98	0.89	0.82
Surface_test (R <sup>2</sup> )	0.44	0.54	0.62
Subsoil_CV (RMSE)	0.60	0.82	0.67
Subsoil_test (RMSE)	0.46	0.80	0.49
Subsoil_test (R <sup>2</sup> )	0.43	0.08	0.36

965 **Table S2.** Model performance for predictions of potential soil respiration with physicochemical  
 966 variables (Physicochemistry Model), SOM by NMFk signatures (SOM Model), and combined  
 967 physicochemical variables and SOM variables (Physicochemistry & SOM Model) for average 5-  
 968 fold cross-validation accuracies (training soils, RMSE), and testing sample accuracies (RMSE, R<sup>2</sup>).

969

Hyperparameter name	param_distributions	Physicochemistry Model		SOM Model		Physicochemistry & SOM Model	
		Surface	Subsoil	Surface	subsoil	surface	subsoil
970 n_estimators	randint(50,5000)	1213	1722	422	636	1392	351
971 max_depth	randint(2,60)	31	58	14	7	40	16
972 max_features	randint(1, X.shape[1])	1	6	2	5	3	7
973							
974 min_samples_split	randint(2, 10)	6	6	4	6	7	9
975 learning_rate	[0.0001, 0.001, 0.01, 0.1, 1.0]	0.01	0.01	0.1	0.001	0.1	0.1
976							
977 ccp_alpha	expon(scale=0.1)	9.42e-4	0.0173	0.0435	1.77e-3	1.86e-5	6.59e-4

978

979 **Table S3.** Hyperparameter tuning settings and the tuned hyperparameters used in each model.

980



## 981 References in Supporting Information

- 982
- 983
- 984 Allison, S. (2012). A trait-based approach for modelling microbial litter decomposition. *Ecology letters*, *15*(9),
- 985 1058-1070.
- 986 Amador, J., & Jones, R. D. (1993). Nutrient limitations on microbial respiration in peat soils with different total
- 987 phosphorus content. *Soil Biology and Biochemistry*, *25*(6), 793-801.
- 988 Angst, G., Mueller, K. E., Nierop, K. G. J., & Simpson, M. J. (2021). Plant- or microbial-derived? A review on the
- 989 molecular composition of stabilized soil organic matter. *Soil Biology and Biochemistry*, *156*, 108189.
- 990 <https://www.sciencedirect.com/science/article/pii/S0038071721000614>
- 991 AOAC, I. (2006). AOAC Official Method 972.43, Microchemical determination of carbon, hydrogen, and nitrogen,
- 992 automated method. *Official Methods of Analysis of AOAC International*. AOAC International,
- 993 Gaithersburg, MD, 5-6.
- 994 Bahureksa, W., Tfaily, M. M., Boiteau, R. M., Young, R. B., Logan, M. N., McKenna, A. M., & Borch, T. (2021).
- 995 Soil organic matter characterization by Fourier transform ion cyclotron resonance mass spectrometry
- 996 (FTICR MS): A critical review of sample preparation, analysis, and data interpretation. *Environmental*
- 997 *Science & Technology*, *55*(14), 9637-9656.
- 998 Benbi, D., Boparai, A., & Brar, K. (2014). Decomposition of particulate organic matter is more sensitive to
- 999 temperature than the mineral associated organic matter. *Soil Biology and Biochemistry*, *70*, 183-192.
- 1000 Berryman, E. M., Marshall, J. D., & Kavanagh, K. (2014). Decoupling litter respiration from whole-soil respiration
- 1001 along an elevation gradient in a Rocky Mountain mixed-conifer forest. *Canadian Journal of Forest*
- 1002 *Research*, *44*(5), 432-440. <https://cdnsiencepub.com/doi/abs/10.1139/cjfr-2013-0334>
- 1003 Bhattarai, M., Chennupati, G., Skau, E., Vangara, R., Djidjev, H., & Alexandrov, B. S. (2020, 22-24 Sept. 2020).
- 1004 *Distributed Non-Negative Tensor Train Decomposition*. Paper presented at the 2020 IEEE High
- 1005 Performance Extreme Computing Conference (HPEC).
- 1006 Bholowalia, P., & Kumar, A. (2014). EBK-means: A clustering technique based on elbow method and k-means in
- 1007 WSN. *International Journal of Computer Applications*, *105*(9).
- 1008 Billings, S. A., & Ballantyne IV, F. (2013). How interactions between microbial resource demands, soil organic
- 1009 matter stoichiometry, and substrate reactivity determine the direction and magnitude of soil respiratory
- 1010 responses to warming. *Global Change Biology*, *19*(1), 90-102.
- 1011 Billings, S. A., Lajtha, K., Malhotra, A., Berhe, A. A., de Graaff, M. A., Earl, S., et al. (2021). Soil organic carbon is
- 1012 not just for soil scientists: measurement recommendations for diverse practitioners. *Ecological*
- 1013 *Applications*, *31*(3), e02290.
- 1014 Bond-Lamberty, B., & Thomson, A. (2010). Temperature-associated increases in the global soil respiration record.
- 1015 *Nature*, *464*(7288), 579-582.
- 1016 Bowman, M. M., Heath, A. E., Varga, T., Battu, A. K., Chu, R. K., Toyoda, J., et al. (2023). One thousand soils for
- 1017 molecular understanding of belowground carbon cycling. *Frontiers in Soil Science*, *3*. Perspective.
- 1018 <https://www.frontiersin.org/articles/10.3389/fsoil.2023.1120425>
- 1019 Bradford, M. A., Wieder, W. R., Bonan, G. B., Fierer, N., Raymond, P. A., & Crowther, T. W. (2016). Managing
- 1020 uncertainty in soil carbon feedbacks to climate change. *Nature Climate Change*, *6*(8), 751-758.
- 1021 Bradford, M. A., Wood, S. A., Addicott, E. T., Fenichel, E. P., Fields, N., González-Rivero, J., et al. (2021).
- 1022 Quantifying microbial control of soil organic matter dynamics at macrosystem scales. *Biogeochemistry*,
- 1023 *156*(1), 19-40. <https://doi.org/10.1007/s10533-021-00789-5>
- 1024 Bray, R. H., & Kurtz, L. T. (1945). Determination of total, organic, and available forms of phosphorus in soils. *Soil*
- 1025 *science*, *59*(1), 39-46.
- 1026 Brookes, P., Landman, A., Pruden, G., & Jenkinson, D. (1985). Chloroform fumigation and the release of soil
- 1027 nitrogen: a rapid direct extraction method to measure microbial biomass nitrogen in soil. *Soil biology and*
- 1028 *biochemistry*, *17*(6), 837-842.
- 1029 Brye, K. R., McMullen, R. L., Silveira, M. L., Motschenbacher, J. M. D., Smith, S. F., Gbur, E. E., & Helton, M. L.
- 1030 (2016). Environmental controls on soil respiration across a southern US climate gradient: a meta-analysis.
- 1031 *Geoderma Regional*, *7*(2), 110-119. <https://www.sciencedirect.com/science/article/pii/S2352009416300104>
- 1032 Cai, Y., Gu, H., & Kenney, T. (2017). Learning Microbial Community Structures with Supervised and Unsupervised
- 1033 Non-negative Matrix Factorization. *Microbiome*, *5*(1), 110. <https://doi.org/10.1186/s40168-017-0323-1>
- 1034 Camenzind, T., Mason-Jones, K., Mansour, I., Rillig, M. C., & Lehmann, J. (2023). Formation of necromass-derived
- 1035 soil organic carbon determined by microbial death pathways. *Nature Geoscience*, *16*(2), 115-122.
- 1036 <https://doi.org/10.1038/s41561-022-01100-3>

- 1037 Campbell, T. P., Ulrich, D. E. M., Toyoda, J., Thompson, J., Munsky, B., Albright, M. B. N., et al. (2022).  
 1038 Microbial Communities Influence Soil Dissolved Organic Carbon Concentration by Altering Metabolite  
 1039 Composition. *Frontiers in microbiology*, *12*. Original Research.  
 1040 <https://www.frontiersin.org/articles/10.3389/fmicb.2021.799014>
- 1041 Chao, L., Liu, Y., Freschet, G. T., Zhang, W., Yu, X., Zheng, W., et al. (2019). Litter carbon and nutrient chemistry  
 1042 control the magnitude of soil priming effect. *Functional Ecology*, *33*(5), 876-888.
- 1043 Chen, S., Zou, J., Hu, Z., Chen, H., & Lu, Y. (2014). Global annual soil respiration in relation to climate, soil  
 1044 properties and vegetation characteristics: Summary of available data. *Agricultural and Forest Meteorology*,  
 1045 *198-199*, 335-346. <https://www.sciencedirect.com/science/article/pii/S0168192314002159>
- 1046 Christ, M., Braun, N., Neuffer, J., & Kempa-Liehr, A. W. (2018). Time Series Feature Extraction on basis of  
 1047 Scalable Hypothesis tests (tsfresh – A Python package). *Neurocomputing*, *307*, 72-77.  
 1048 <https://www.sciencedirect.com/science/article/pii/S0925231218304843>
- 1049 Ciais, P., Sabine, C., Bala, G., Bopp, L., Brovkin, V., Canadell, J., et al. (2014). Carbon and other biogeochemical  
 1050 cycles. In *Climate change 2013: the physical science basis. Contribution of Working Group I to the Fifth*  
 1051 *Assessment Report of the Intergovernmental Panel on Climate Change* (pp. 465-570): Cambridge  
 1052 University Press.
- 1053 Corbridge, D. E. C. (1980). *Phosphorus. An outline of its chemistry, biochemistry, and technology*: Elsevier  
 1054 Scientific Co.
- 1055 Corilo, Y., Kew, W., & McCue, L. (2021). EMSL-Computing/CoreMS: CoreMS 1.0. 0 (v1. 0.0). *Zenodo**10*, 5281.
- 1056 Cotrufo, M. F., Ranalli, M. G., Haddix, M. L., Six, J., & Lugato, E. (2019). Soil carbon storage informed by  
 1057 particulate and mineral-associated organic matter. *Nature Geoscience*, *12*(12), 989-994.
- 1058 Cotrufo, M. F., Wallenstein, M. D., Boot, C. M., Denef, K., & Paul, E. (2013). The Microbial Efficiency-Matrix S  
 1059 tabilization (MEMS) framework integrates plant litter decomposition with soil organic matter stabilization:  
 1060 Do labile plant inputs form stable soil organic matter? *Global change biology*, *19*(4), 988-995.
- 1061 Crowther, T. W., Todd-Brown, K. E. O., Rowe, C. W., Wieder, W. R., Carey, J. C., Machmuller, M. B., et al.  
 1062 (2016). Quantifying global soil carbon losses in response to warming. *Nature*, *540*(7631), 104-108.  
 1063 <https://doi.org/10.1038/nature20150>
- 1064 Curiel Yuste, J., Baldocchi, D., Gershenson, A., Goldstein, A., Misson, L., & Wong, S. (2007). Microbial soil  
 1065 respiration and its dependency on carbon inputs, soil temperature and moisture. *Global Change Biology*,  
 1066 *13*(9), 2018-2035.
- 1067 Davenport, R., Bowen, B. P., Lynch, L. M., Kosina, S. M., Shabtai, I., Northen, T. R., & Lehmann, J. (2023).  
 1068 Decomposition decreases molecular diversity and ecosystem similarity of soil organic matter. *Proceedings*  
 1069 *of the National Academy of Sciences*, *120*(25), e2303335120.  
 1070 <https://www.pnas.org/doi/abs/10.1073/pnas.2303335120>
- 1071 Davidson, E. A., & Janssens, I. A. (2006). Temperature sensitivity of soil carbon decomposition and feedbacks to  
 1072 climate change. *Nature*, *440*(7081), 165-173.
- 1073 Devarajan, K. (2008). Nonnegative Matrix Factorization: An Analytical and Interpretive Tool in Computational  
 1074 Biology. *PLOS Computational Biology*, *4*(7), e1000029. <https://doi.org/10.1371/journal.pcbi.1000029>
- 1075 Dittmar, T., Koch, B., Hertkorn, N., & Kattner, G. (2008). A simple and efficient method for the solid-phase  
 1076 extraction of dissolved organic matter (SPE-DOM) from seawater. *Limnology and Oceanography: Methods*,  
 1077 *6*(6), 230-235. <https://aslopubs.onlinelibrary.wiley.com/doi/abs/10.4319/lom.2008.6.230>
- 1078 Elser, J., Sterner, R., Gorokhova, E. a., Fagan, W., Markow, T., Cotner, J., et al. (2000). Biological stoichiometry  
 1079 from genes to ecosystems. *Ecology letters*, *3*(6), 540-550.
- 1080 Falloon, P., Jones, C. D., Ades, M., & Paul, K. (2011). Direct soil moisture controls of future global soil carbon  
 1081 changes: An important source of uncertainty. *Global Biogeochemical Cycles*, *25*(3).
- 1082 Fan, B., Yin, L., Dijkstra, F. A., Lu, J., Shao, S., Wang, P., et al. (2022). Potential gross nitrogen mineralization and  
 1083 its linkage with microbial respiration along a forest transect in eastern China. *Applied Soil Ecology*, *171*,  
 1084 104347. <https://www.sciencedirect.com/science/article/pii/S0929139321004704>
- 1085 Fang, C., & Moncrieff, J. B. (2005). The variation of soil microbial respiration with depth in relation to soil carbon  
 1086 composition. *Plant and Soil*, *268*(1), 243-253. <https://doi.org/10.1007/s11104-004-0278-4>
- 1087 Fang, C., & Moncrieff, J. B. (2005). The variation of soil microbial respiration with depth in relation to soil carbon  
 1088 composition. *Plant and Soil*, *268*, 243-253.
- 1089 Friedlingstein, P., O'Sullivan, M., Jones, M. W., Andrew, R. M., Gregor, L., Hauck, J., et al. (2022). Global Carbon  
 1090 Budget 2022. *Earth Syst. Sci. Data*, *14*(11), 4811-4900. <https://essd.copernicus.org/articles/14/4811/2022/>
- 1091 Friedman, J. H. (2001). Greedy function approximation: a gradient boosting machine. *Annals of statistics*, 1189-  
 1092 1232.

- 1093 Garayburu-Caruso, V. A., Stegen, J. C., Song, H.-S., Renteria, L., Wells, J., Garcia, W., et al. (2020). Carbon  
 1094 limitation leads to thermodynamic regulation of aerobic metabolism. *Environmental Science & Technology*  
 1095 *Letters*, 7(7), 517-524.
- 1096 Giardina, C. P., Litton, C. M., Crow, S. E., & Asner, G. P. (2014). Warming-related increases in soil CO<sub>2</sub> efflux are  
 1097 explained by increased below-ground carbon flux. *Nature Climate Change*, 4(9), 822-827.  
 1098 <https://doi.org/10.1038/nclimate2322>
- 1099 Graham, E. B., Crump, A. R., Kennedy, D. W., Arntzen, E., Fansler, S., Purvine, S. O., et al. (2018). Multi'omics  
 1100 comparison reveals metabolome biochemistry, not microbiome composition or gene expression,  
 1101 corresponds to elevated biogeochemical function in the hyporheic zone. *Science of the total environment*,  
 1102 642, 742-753.
- 1103 Graham, E. B., & Hofmockel, K. S. (2022). Ecological stoichiometry as a foundation for omics-enabled  
 1104 biogeochemical models of soil organic matter decomposition. *Biogeochemistry*, 157(1), 31-50.
- 1105 Graham, E. B., Wieder, W. R., Leff, J. W., Weintraub, S. R., Townsend, A. R., Cleveland, C. C., et al. (2014). Do  
 1106 we need to understand microbial communities to predict ecosystem function? A comparison of statistical  
 1107 models of nitrogen cycling processes. *Soil Biology and Biochemistry*, 68, 279-282.
- 1108 Gransee, A., & Führs, H. (2013). Magnesium mobility in soils as a challenge for soil and plant analysis, magnesium  
 1109 fertilization and root uptake under adverse growth conditions. *Plant and Soil*, 368(1), 5-21.  
 1110 <https://doi.org/10.1007/s11104-012-1567-y>
- 1111 Guillaumet, D., & Vitria, J. (2002). *Non-negative matrix factorization for face recognition*. Paper presented at the  
 1112 Catalonian Conference on Artificial Intelligence.
- 1113 Hall, S. J., Ye, C., Weintraub, S. R., & Hockaday, W. C. (2020). Molecular trade-offs in soil organic carbon  
 1114 composition at continental scale. *Nature Geoscience*, 13(10), 687-692. [https://doi.org/10.1038/s41561-020-](https://doi.org/10.1038/s41561-020-0634-x)  
 1115 0634-x
- 1116 Hastie, T., Tibshirani, R., Friedman, J. H., & Friedman, J. H. (2009). *The elements of statistical learning: data*  
 1117 *mining, inference, and prediction* (Vol. 2): Springer.
- 1118 Hernández, D. L., & Hobbie, S. E. (2010). The effects of substrate composition, quantity, and diversity on microbial  
 1119 activity. *Plant and Soil*, 335(1), 397-411. <https://doi.org/10.1007/s11104-010-0428-9>
- 1120 Huys, R., Poirier, V., Bourget, M. Y., Roumet, C., Hättenschwiler, S., Fromin, N., et al. (2022). Plant litter  
 1121 chemistry controls coarse-textured soil carbon dynamics. *Journal of Ecology*, 110(12), 2911-2928.
- 1122 Jian, J., Vargas, R., Anderson-Teixeira, K., Stell, E., Herrmann, V., Horn, M., et al. (2021). A restructured and  
 1123 updated global soil respiration database (SRDB-V5). *Earth Syst. Sci. Data*, 13(2), 255-267.  
 1124 <https://essd.copernicus.org/articles/13/255/2021/>
- 1125 Johnson, G. W., Ehrlich, R., Full, W., & Ramos, S. (2015). Principal components analysis and receptor models in  
 1126 environmental forensics. In *Introduction to environmental forensics* (pp. 609-653): Elsevier.
- 1127 Jones, D. L. (1999). Amino acid biodegradation and its potential effects on organic nitrogen capture by plants. *Soil*  
 1128 *biology and biochemistry*, 31(4), 613-622.
- 1129 Kallenbach, C. M., Frey, S. D., & Grandy, A. S. (2016). Direct evidence for microbial-derived soil organic matter  
 1130 formation and its ecophysiological controls. *Nature Communications*, 7(1), 13630.  
 1131 <https://doi.org/10.1038/ncomms13630>
- 1132 Kim, S., Kramer, R. W., & Hatcher, P. G. (2003). Graphical method for analysis of ultrahigh-resolution broadband  
 1133 mass spectra of natural organic matter, the van Krevelen diagram. *Analytical chemistry*, 75(20), 5336-5344.
- 1134 Kögel-Knabner, I. (2002). The macromolecular organic composition of plant and microbial residues as inputs to soil  
 1135 organic matter. *Soil Biology and Biochemistry*, 34(2), 139-162.  
 1136 <https://www.sciencedirect.com/science/article/pii/S0038071701001584>
- 1137 Kramer, C., & Gleixner, G. (2008). Soil organic matter in soil depth profiles: Distinct carbon preferences of  
 1138 microbial groups during carbon transformation. *Soil Biology and Biochemistry*, 40(2), 425-433.  
 1139 <https://www.sciencedirect.com/science/article/pii/S0038071707003768>
- 1140 Kranabetter, J. M., Philpott, T., & Dunn, D. (2021). Manganese limitations and the enhanced soil carbon  
 1141 sequestration of temperate rainforests. *Biogeochemistry*, 156(2), 195-209.
- 1142 Kyker-Snowman, E., Wieder, W. R., Frey, S. D., & Grandy, A. S. (2020). Stoichiometrically coupled carbon and  
 1143 nitrogen cycling in the MICROBIAL-MINERAL CARBON STABILIZATION model version 1.0 (MIMICS-CN v1.0).  
 1144 *Geoscientific Model Development*, 13(9), 4413-4434.
- 1145 Lee, D., & Seung, H. S. (2000). Algorithms for non-negative matrix factorization. *Advances in neural information*  
 1146 *processing systems*, 13.

- 1147 Lee, K.-H., & Jose, S. (2003). Soil respiration, fine root production, and microbial biomass in cottonwood and  
 1148 loblolly pine plantations along a nitrogen fertilization gradient. *Forest Ecology and Management*, 185(3),  
 1149 263-273. <https://www.sciencedirect.com/science/article/pii/S0378112703001646>
- 1150 Lehmann, J., Hansel, C. M., Kaiser, C., Kleber, M., Maher, K., Manzoni, S., et al. (2020). Persistence of soil organic  
 1151 carbon caused by functional complexity. *Nature Geoscience*, 13(8), 529-534.  
 1152 <https://doi.org/10.1038/s41561-020-0612-3>
- 1153 Lei, J., Guo, X., Zeng, Y., Zhou, J., Gao, Q., & Yang, Y. (2021). Temporal changes in global soil respiration since  
 1154 1987. *Nature communications*, 12(1), 403.
- 1155 Li, H., Santos, F., Butler, K., & Herndon, E. (2021). A critical review on the multiple roles of manganese in  
 1156 stabilizing and destabilizing soil organic matter. *Environmental Science & Technology*, 55(18), 12136-  
 1157 12152.
- 1158 Liang, C., Amelung, W., Lehmann, J., & Kästner, M. (2019). Quantitative assessment of microbial necromass  
 1159 contribution to soil organic matter. *Global change biology*, 25(11), 3578-3590.
- 1160 Lugato, E., Lavalley, J. M., Haddix, M. L., Panagos, P., & Cotrufo, M. F. (2021). Different climate sensitivity of  
 1161 particulate and mineral-associated soil organic matter. *Nature Geoscience*, 14(5), 295-300.
- 1162 Marschner, B., & Kalbitz, K. (2003). Controls of bioavailability and biodegradability of dissolved organic matter in  
 1163 soils. *Geoderma*, 113(3-4), 211-235.
- 1164 Melillo, J. M., Frey, S. D., DeAngelis, K. M., Werner, W. J., Bernard, M. J., Bowles, F. P., et al. (2017). Long-term  
 1165 pattern and magnitude of soil carbon feedback to the climate system in a warming world. *Science*,  
 1166 358(6359), 101-105.
- 1167 Mori, T., Lu, X., Aoyagi, R., & Mo, J. (2018). Reconsidering the phosphorus limitation of soil microbial activity in  
 1168 tropical forests. *Functional Ecology*, 32(5), 1145-1154.
- 1169 Moyano, F. E., Manzoni, S., & Chenu, C. (2013). Responses of soil heterotrophic respiration to moisture  
 1170 availability: An exploration of processes and models. *Soil Biology and Biochemistry*, 59, 72-85.
- 1171 Neupane, A., Herndon, E. M., Whitman, T., Faiia, A. M., & Jagadamma, S. (2023). Manganese effects on plant  
 1172 residue decomposition and carbon distribution in soil fractions depend on soil nitrogen availability. *Soil  
 1173 Biology and Biochemistry*, 178, 108964.
- 1174 Nicolás, C., Martin-Bertelsen, T., Floudas, D., Bentzer, J., Smits, M., Johansson, T., et al. (2019). The soil organic  
 1175 matter decomposition mechanisms in ectomycorrhizal fungi are tuned for liberating soil organic nitrogen.  
 1176 *The ISME journal*, 13(4), 977-988. <https://doi.org/10.1038/s41396-018-0331-6>
- 1177 Nissan, A., Alcolombri, U., Peleg, N., Galili, N., Jimenez-Martinez, J., Molnar, P., & Holzner, M. (2023). Global  
 1178 warming accelerates soil heterotrophic respiration. *Nature communications*, 14(1), 3452.
- 1179 Opfergelt, S., Cornélis, J. T., Houben, D., Givron, C., Burton, K. W., & Mattielli, N. (2017). The influence of  
 1180 weathering and soil organic matter on Zn isotopes in soils. *Chemical Geology*, 466, 140-148.  
 1181 <https://www.sciencedirect.com/science/article/pii/S0009254117303601>
- 1182 Orchard, V. A., & Cook, F. (1983). Relationship between soil respiration and soil moisture. *Soil Biology and  
 1183 Biochemistry*, 15(4), 447-453.
- 1184 Paatero, P., & Tapper, U. (1994). Positive matrix factorization: A non-negative factor model with optimal utilization  
 1185 of error estimates of data values. *Environmetrics*, 5(2), 111-126.
- 1186 Pauca, V. P., Shahnaz, F., Berry, M. W., & Plemmons, R. J. (2004). *Text mining using non-negative matrix  
 1187 factorizations*. Paper presented at the Proceedings of the 2004 SIAM international conference on data  
 1188 mining.
- 1189 Raich, J. W., & Potter, C. S. (1995). Global patterns of carbon dioxide emissions from soils. *Global biogeochemical  
 1190 cycles*, 9(1), 23-36.
- 1191 Raich, J. W., Potter, C. S., & Bhagawati, D. (2002). Interannual variability in global soil respiration, 1980-94.  
 1192 *Global Change Biology*, 8(8), 800-812.
- 1193 Riaz, M., & Marschner, P. (2020). Sandy Soil Amended with Clay Soil: Effect of Clay Soil Properties on Soil  
 1194 Respiration, Microbial Biomass, and Water Extractable Organic C. *Journal of Soil Science and Plant  
 1195 Nutrition*, 20(4), 2465-2470. <https://doi.org/10.1007/s42729-020-00312-z>
- 1196 Robertson, A. D., Paustian, K., Ogle, S., Wallenstein, M. D., Lugato, E., & Cotrufo, M. F. (2019). Unifying soil  
 1197 organic matter formation and persistence frameworks: the MEMS model. *Biogeosciences*, 16(6), 1225-  
 1198 1248.
- 1199 Rodenburg, L. A., Du, S., Xiao, B., & Fennell, D. E. (2011). Source apportionment of polychlorinated biphenyls in  
 1200 the New York/New Jersey Harbor. *Chemosphere*, 83(6), 792-798.

- 1201 Roth, V.-N., Lange, M., Simon, C., Hertkorn, N., Bucher, S., Goodall, T., et al. (2019). Persistence of dissolved  
1202 organic matter explained by molecular changes during its passage through soil. *Nature Geoscience*, *12*(9),  
1203 755-761. <https://doi.org/10.1038/s41561-019-0417-4>
- 1204 Rumpel, C., & Kögel-Knabner, I. (2011). Deep soil organic matter—a key but poorly understood component of  
1205 terrestrial C cycle. *Plant and soil*, *338*, 143-158.
- 1206 Sanderman, J., Baldock, J. A., Dangal, S. R. S., Ludwig, S., Potter, S., Rivard, C., & Savage, K. (2021). Soil organic  
1207 carbon fractions in the Great Plains of the United States: an application of mid-infrared spectroscopy.  
1208 *Biogeochemistry*, *156*(1), 97-114. <https://doi.org/10.1007/s10533-021-00755-1>
- 1209 Santos, F., & Herndon, E. (2023). Plant-Soil Relationships Influence Observed Trends Between Manganese and  
1210 Carbon Across Biomes. *Global Biogeochemical Cycles*, *37*(1), e2022GB007412.
- 1211 Schimel, J. (2021). The Democracy of dirt: relating micro-scale dynamics to macro-scale ecosystem function.  
1212 *Microbes: The foundation stone of the biosphere*, 89-102.
- 1213 Scott, N. A., Cole, C. V., Elliott, E. T., & Huffman, S. A. (1996). Soil textural control on decomposition and soil  
1214 organic matter dynamics. *Soil Science Society of America Journal*, *60*(4), 1102-1109.
- 1215 Siles, J. A., Cajthaml, T., Filipová, A., Minerbi, S., & Margesin, R. (2017). Altitudinal, seasonal and interannual  
1216 shifts in microbial communities and chemical composition of soil organic matter in Alpine forest soils. *Soil*  
1217 *Biology and Biochemistry*, *112*, 1-13.  
1218 <https://www.sciencedirect.com/science/article/pii/S0038071716305600>
- 1219 Song, H.-S., Stegen, J. C., Graham, E. B., Lee, J.-Y., Garayburu-Caruso, V. A., Nelson, W. C., et al. (2020).  
1220 Representing organic matter thermodynamics in biogeochemical reactions via substrate-explicit modeling.  
1221 *Frontiers in microbiology*, *11*, 531756.
- 1222 Sonnewald, M., Dutkiewicz, S., Hill, C., & Forget, G. (2020). Elucidating ecological complexity: Unsupervised  
1223 learning determines global marine eco-provinces. *Science Advances*, *6*(22), eaay4740.  
1224 <https://www.science.org/doi/abs/10.1126/sciadv.aay4740>
- 1225 Soong, J. L., Fuchslueger, L., Maraňon-Jimenez, S., Torn, M. S., Janssens, I. A., Penuelas, J., & Richter, A. (2020).  
1226 Microbial carbon limitation: The need for integrating microorganisms into our understanding of ecosystem  
1227 carbon cycling. *Global change biology*, *26*(4), 1953-1961.
- 1228 Subedi, P., Jokela, E. J., Vogel, J. G., Bracho, R., & Inglett, K. S. (2021). The effects of nutrient limitations on  
1229 microbial respiration and organic matter decomposition in a Florida Spodosol as influenced by historical  
1230 forest management practices. *Forest Ecology and Management*, *479*, 118592.
- 1231 Sulman, B. N., Phillips, R. P., Oishi, A. C., Shevliakova, E., & Pacala, S. W. (2014). Microbe-driven turnover  
1232 offsets mineral-mediated storage of soil carbon under elevated CO<sub>2</sub>. *Nature Climate Change*, *4*(12), 1099-  
1233 1102.
- 1234 Taylor, P. G., & Townsend, A. R. (2010). Stoichiometric control of organic carbon–nitrate relationships from soils  
1235 to the sea. *Nature*, *464*(7292), 1178-1181. <https://doi.org/10.1038/nature08985>
- 1236 Tfaily, M. M., Chu, R. K., Tolić, N., Roscioli, K. M., Anderton, C. R., Paša-Tolić, L., et al. (2015). Advanced  
1237 solvent based methods for molecular characterization of soil organic matter by high-resolution mass  
1238 spectrometry. *Analytical chemistry*, *87*(10), 5206-5215.
- 1239 Todd-Brown, K., Randerson, J., Hopkins, F., Arora, V., Hajima, T., Jones, C., et al. (2014). Changes in soil organic  
1240 carbon storage predicted by Earth system models during the 21st century. *Biogeosciences*, *11*(8), 2341-  
1241 2356.
- 1242 Turețcaia, A. B., Garayburu-Caruso, V. A., Kaufman, M. H., Danczak, R. E., Stegen, J. C., Chu, R. K., et al. (2023).  
1243 Rethinking Aerobic Respiration in the Hyporheic Zone under Variation in Carbon and Nitrogen  
1244 Stoichiometry. *Environmental Science & Technology*, *57*(41), 15499-15510.  
1245 <https://doi.org/10.1021/acs.est.3c04765>
- 1246 Vangara, R., Bhattarai, M., Skau, E., Chennupati, G., Djidjev, H., Tierney, T., et al. (2021). Finding the Number of  
1247 Latent Topics With Semantic Non-Negative Matrix Factorization. *IEEE Access*, *9*, 117217-117231.
- 1248 Vesselinov, V. V., Alexandrov, B. S., & O'Malley, D. (2018). Contaminant source identification using semi-  
1249 supervised machine learning. *Journal of Contaminant Hydrology*, *212*, 134-142.  
1250 <https://www.sciencedirect.com/science/article/pii/S0169772217301201>
- 1251 Wang, Y.-P., & Houlton, B. Z. (2009). Nitrogen constraints on terrestrial carbon uptake: Implications for the global  
1252 carbon-climate feedback. *Geophysical Research Letters*, *36*(24).  
1253 <https://agupubs.onlinelibrary.wiley.com/doi/abs/10.1029/2009GL041009>
- 1254 Waring, B. G., Sulman, B. N., Reed, S., Smith, A. P., Averill, C., Creamer, C. A., et al. (2020). From pools to flow:  
1255 The PROMISE framework for new insights on soil carbon cycling in a changing world. *Global Change*  
1256 *Biology*, *26*(12), 6631-6643.

- 1257 Warner, D., Bond-Lamberty, B., Jian, J., Stell, E., & Vargas, R. (2019). Spatial predictions and associated  
1258 uncertainty of annual soil respiration at the global scale. *Global Biogeochemical Cycles*, 33(12), 1733-  
1259 1745.
- 1260 Whalen, E. D. (2017). *Manganese Limitation as a Mechanism for Reduced Decomposition in Soils under Long-*  
1261 *Term Atmospheric Nitrogen Deposition*. University of New Hampshire,
- 1262 Wieder, W. R., Hartman, M. D., Sulman, B. N., Wang, Y. P., Koven, C. D., & Bonan, G. B. (2018). Carbon cycle  
1263 confidence and uncertainty: Exploring variation among soil biogeochemical models. *Global change*  
1264 *biology*, 24(4), 1563-1579.
- 1265 Witt, C., Gaunt, J. L., Galicia, C. C., Ottow, J. C., & Neue, H.-U. (2000). A rapid chloroform-fumigation extraction  
1266 method for measuring soil microbial biomass carbon and nitrogen in flooded rice soils. *Biology and*  
1267 *Fertility of Soils*, 30, 510-519.
- 1268 Witzgall, K., Vidal, A., Schubert, D. I., Höschen, C., Schweizer, S. A., Buegger, F., et al. (2021). Particulate organic  
1269 matter as a functional soil component for persistent soil organic carbon. *Nature Communications*, 12(1),  
1270 4115.
- 1271 Xu, L., Baldocchi, D. D., & Tang, J. (2004). How soil moisture, rain pulses, and growth alter the response of  
1272 ecosystem respiration to temperature. *Global Biogeochemical Cycles*, 18(4).
- 1273 Yuan, B., Tan, Y. J., Mudunuru, M. K., Marcillo, O. E., Delorey, A. A., Roberts, P. M., et al. (2019). Using  
1274 Machine Learning to Discern Eruption in Noisy Environments: A Case Study Using CO<sub>2</sub>-Driven Cold-  
1275 Water Geyser in Chimayó, New Mexico. *Seismological Research Letters*, 90(2A), 591-603.  
1276 <https://doi.org/10.1785/0220180306>
- 1277 Zhang, H., Goll, D. S., Wang, Y. P., Ciais, P., Wieder, W. R., Abramoff, R., et al. (2020). Microbial dynamics and  
1278 soil physicochemical properties explain large-scale variations in soil organic carbon. *Global Change*  
1279 *Biology*, 26(4), 2668-2685.
- 1280 Zhang, M., Zhang, X., Zhang, L., Zeng, L., Liu, Y., Wang, X., et al. (2021). The stronger impact of inorganic  
1281 nitrogen fertilization on soil bacterial community than organic fertilization in short-term condition.  
1282 *Geoderma*, 382, 114752. <https://www.sciencedirect.com/science/article/pii/S0016706120325076>
- 1283 Zhao, Q., Callister, S. J., Thompson, A. M., Kukkadapu, R. K., Tfaily, M. M., Bramer, L. M., et al. (2020). Strong  
1284 mineralogic control of soil organic matter composition in response to nutrient addition across diverse  
1285 grassland sites. *Science of The Total Environment*, 736, 137839.  
1286 <https://www.sciencedirect.com/science/article/pii/S0048969720313516>
- 1287 Zhao, Q., Thompson, A. M., Callister, S. J., Tfaily, M. M., Bell, S. L., Hobbie, S. E., & Hofmockel, K. S. (2022).  
1288 Dynamics of organic matter molecular composition under aerobic decomposition and their response to the  
1289 nitrogen addition in grassland soils. *Science of the Total Environment*, 806, 150514.
- 1290